Solving spin quantum master equations with matrix continued-fraction methods: application to superparamagnets

Solving spin quantum master equations with matrix continued-fraction methods: application to superparamagnets

J L García-Palacios and D Zueco

Departamento de Física de la Materia Condensada e Instituto de Ciencia de Materiales de Aragón, CSIC–Universidad de Zaragoza, E-50009 Zaragoza, Spain

Abstract
We implement continued-fraction techniques to solve exactly quantum master equations for a spin with arbitrary S coupled to a (bosonic) thermal bath. The full spin density matrix is obtained, so that along with relaxation and thermoactivation, coherent dynamics is included (precession, tunnel, etc). The method is applied to study isotropic spins and spins in a bistable anisotropy potential (superparamagnets). We present examples of static response, the dynamical susceptibility including the contribution of different relaxation modes, and of spin resonance in transverse fields.

PACS numbers: 03.65.Yz, 05.40.−a, 76.20.+q, 75.50.Xx

1. Introduction

In the field of *quantum dissipative systems* one studies a subsystem consisting of a few relevant degrees of freedom coupled to the surrounding medium (bath), which has a large number of constituents (e.g., photons, phonons, electrons, nuclei) [1–3]. The (sub)system is not necessarily microscopic, but it can be a mesoscopic system (a Josephson junction, a magnetic molecular cluster, etc) described by a few *collective* variables (phase across the junction, net spin) which under certain conditions can display quantum behaviour. Various fundamental problems can be addressed, such as dissipation and quantum mechanics, decoherence, quantum Brownian motion, or the quantum-to-classical transition. The interaction with the bath, apart from producing dissipation, fluctuations and decoherence, enables the system to interchange energy, momentum and correlations with its environment and eventually relax to thermal equilibrium. For these reasons, the study of open quantum systems is of interest in many areas of physics and chemistry.

Classical open systems are handled as stochastic systems by means of Langevin and Fokker–Planck equations [4]. This approach provides both a theoretical frame and computational tools, e.g., Langevin molecular-dynamics simulations. For few-variable

systems, a powerful technique to solve Fokker–Planck equations is Risken's *continued-fraction method* [4] (a relative of Grad's moment approach for solving kinetic equations [5]). The non-equilibrium distribution W is expanded in a basis of functions and the coupled equations for the expansion coefficients C_i derived. An appropriate basis choice can render finite the coupling range (e.g., with the equation for C_i involving C_{i-1}, C_i and C_{i+1}). Then these recurrences can be solved by iterating a simple algorithm, which has a structure akin to a continued fraction. This method provides numerically exact results in problems of Brownian motion in external potentials, where closed form solutions are scarce (such classical problems are structurally similar to solve a Schrödinger-type equation).

It turns out to be more delicate to deal with *quantum* dissipative systems [1]. First, phenomenological or non-standard quantization poses problems with basic quantum-mechanical principles [6]. Thus, one has to model the environment in a simple way (set of oscillators, 2-state systems, etc), quantize it together with the system, and eventually trace over the bath variables. However, the resulting reduced descriptions are difficult to manage except in simple cases—free particle (or in a uniform field), harmonic oscillator and few-state systems (e.g., $S = 1/2$ spins). In general, the exact *path-integral* expressions for the (reduced) density operator $\varrho(t)$ are not easy to handle [7, 8]; additionally, the propagating function is highly oscillatory, rendering numerical methods unstable at long times [9]. *Quantum Langevin equations* (Heisenberg equations for x and p including operator fluctuations) are of limited use beyond linear systems [10, 11]. Finally, under certain conditions (typically a weak system–bath coupling), the density matrix obeys a *quantum master equation* [12, 13]. But again these equations can only be solved in a few problems.

Due to their performance in classical systems (both translational [14, 15] and rotational [16]), continued-fraction techniques were adapted to several problems of quantum Brownian motion in non-trivial potentials. This was done exploiting pseudo-probability representations of ϱ [17]. Shibata and coworkers [18] applied continued fractions to solve master equations for isotropic spins ($\mathcal{H} = -B_z S_z$); Vogel and Risken tackled similarly quantum non-linear optical problems [19]. In phase-space problems, using the Wigner representation of ϱ, the continued-fraction method for the Klein–Kramers equation was adapted [20] to quantum master equations of Caldeira–Leggett type [6, 21] (explicit recurrences were presented for polynomial and periodic potentials). As these approaches do not rely on the Hamiltonian eigenstructure they are applicable to demanding problems with a (partially) continuous spectrum.

Here we consider the following quantum dissipative system: a spin in the magnetic anisotropy potential $\left(\mathcal{H} = -D S_z^2 - \boldsymbol{B} \cdot \boldsymbol{S}\right)$ coupled to a boson (or bosonizable) thermal bath. For $D = 0$ we recover the familiar isotropic spin with its equispaced Zeeman spectrum; in a sense, the rotational equivalent of the harmonic oscillator. The anisotropy term $-D S_z^2$ makes the problem tougher, say, the spin analogue of Brownian motion in double-well or periodic potentials. The environmental disturbances may indeed provoke a Brownian-type 'reversal' of the spin, overcoming the potential barriers (figure 1). In spite of the analogies, however, dissipative spin dynamics presents essential differences with translational problems, due to the underlying angular-momentum commutation relations $[S_i, S_j] = \mathrm{i}\, \epsilon_{ijk} S_k$ [22–24].

Our Hamiltonian describes paramagnets and superparamagnets—small solids or clusters with a sizable net spin ($S \sim 10^1$–10^4). For large S the physics is approximately classical (as in magnetic nanoparticles) and described by a *rotational* Fokker–Planck equation after Brown [25] and Kubo–Hashitsume [26]. As the spin decreases, quantum effects come to the fore, as in magnetic molecular clusters where $S \sim 5$–25 [27]. The discreteness of the energy levels sensibly affects the thermoactivation processes, while the spin reversal may also occur by tunnelling when the field brings in resonance states at both sides of the barrier (figure 1). An appealing dynamical description is given by master equations of *Pauli* type, for the diagonal
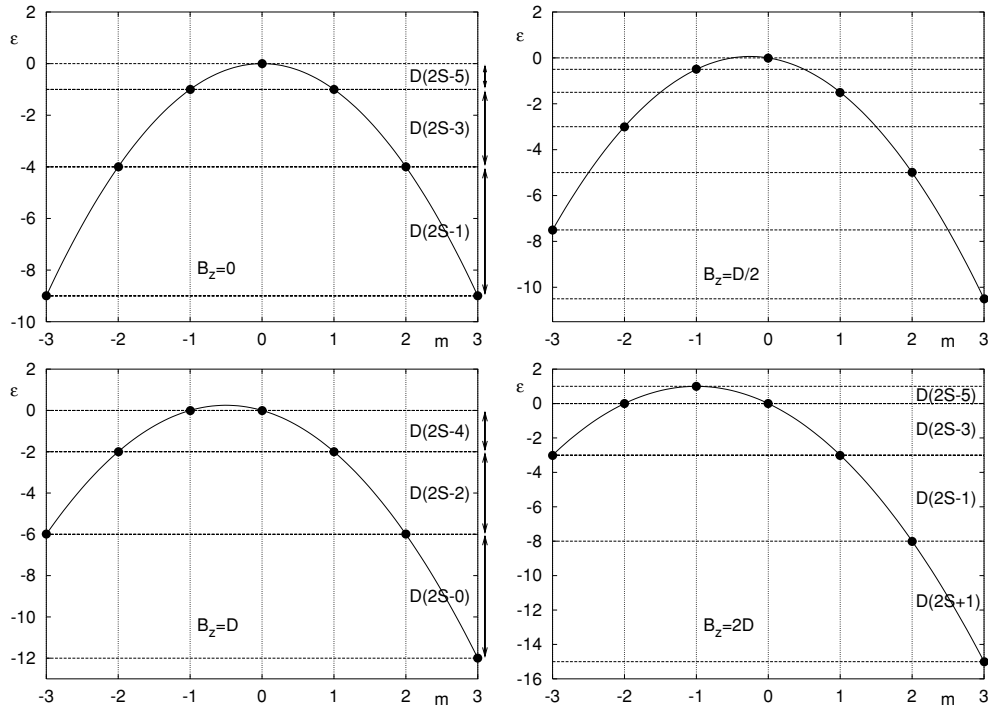
Figure 1. Bistable energy levels of an anisotropic spin, $\varepsilon_m = -Dm^2 - B_z m$, with $S = 3$ and $D = 1$ at zero field (top left). An external field lifts the degeneracy $\varepsilon_{-m} = \varepsilon_m$ (top right). Degeneracies are restored at multiples of D (lower panels).

elements of ϱ ('balance' or 'gain–loss' equations) [11, 28]. These provide some insight, while more refined treatments are less intuitive and difficult to apply. Nevertheless, to take into account *coherent* dynamics, like tunnel oscillations or the spin precession, one also needs off-diagonal density-matrix elements. But, as usual, solving the master equations for the full density matrix is not easy and several (often drastic) simplifications are required.

In this work, following the spirit of [18–20], we will solve master equations for non-interacting spins in contact with a dissipative bath by means of continued-fraction techniques. Exact methods available are limited to small spins ($S \lesssim 5$–10 [29]). Our aim is to tackle arbitrary S, from the extreme quantum cases, $S = 1/2$ and 1, to values as close as possible to the classical domain. This approach differs from those giving some continued-fraction expression for a certain quantity (typically relying on linear-response theory; see the review [30]), in that here the *full solution* of the density-matrix equation is obtained by *matrix* continued-fraction methods. In this theoretical-computational frame we can study spins in a wide range of S ($\lesssim 100$–200) including their full dynamics: relaxation and thermoactivation, precession and coherence, as well as their possible interplay.

The paper is organized as follows. We discuss the isolated spin and present the basic formalism in the next section. In section 3 we introduce dissipative equations for a spin coupled to a bosonic bath, following the compact approach of Garanin *et al* [31, 32] with Heisenberg equations of motion for the Hubbard operators $X_n^m = |n\rangle\langle m|$. Master equations in the Markovian regime are discussed in section 4 and fully specified for several spin problems in section 5. In section 6 we derive the chain of equations resulting from the perturbative treatment

of probing fields (applicable to the non-linear response). In section 7 we manipulate the index-coupling structure of the density-matrix equations to obtain few-term recurrences suitable for implementing the continued-fraction algorithm. Numerous examples of its application to isotropic and anisotropic spins (superparamagnets) are given in sections 8 and 9; we will check the results against exact formulae, whenever possible, and test heuristic expressions. We conclude with an assessment of our approach in section 10 and putting some auxiliary material and discussing technical issues in the appendices.

2. Isolated spin (unitary dynamics) and Hubbard formalism

Our starting point is a spin Hamiltonian [28, 33] including a magnetic anisotropy term and the Zeeman coupling to the field (units $\hbar = k_B = g\mu_B = 1$)

$$\mathcal{H}(\boldsymbol{S}) = -DS_z^2 - \boldsymbol{B} \cdot \boldsymbol{S}. \tag{1}$$

This is the minimal model capturing the physics of (super)paramagnets. The term $-DS_z^2$ has a bistable structure (for $D > 0$) with minima at $S_z = \pm S$ and the barrier top at $S_z = 0$ (figure 1). Along with potential barriers (and degeneracies), an important consequence of the anisotropy is an unequally spaced energy spectrum (appendix A)[1].

Let us introduce the Hubbard (level-shift) operators [35, chapter 1]

$$X_n^m \equiv |n\rangle\langle m|. \tag{2}$$

They form a complete system and any spin operator A can be expressed as

$$A = \sum_{nm} A_{nm} X_n^m, \qquad A_{nm} = \langle n|A|m\rangle. \tag{3}$$

The expansion coefficients are simply the matrix elements of A in the basis defining X_n^m. (If not restricting ourselves to a multiplet with fixed S, we just need to introduce the corresponding indices $|Sm\rangle$ and sum over them.) In particular, for the components of the spin operator one has $S_i = \sum_{nm} \langle n|S_i|m\rangle X_n^m$. Now, if we use the *standard basis* of eigenstates of $\boldsymbol{S}^2$ and S_z, the required matrix elements are $\langle n|S_z|m\rangle = m\delta_{nm}$ and $\langle n|S_\pm|m\rangle = \ell_m^\pm \delta_{n,m\pm1}$. Here $S_\pm = S_x \pm iS_y$ are the ladder operators and $\ell_m^\pm = [S(S+1) - m(m\pm1)]^{1/2}$ the factors giving $S_\pm|m\rangle = \ell_m^\pm|m\pm1\rangle$. Then, S_i are represented by the single-sum forms

$$S_z = \sum_m m X_m^m, \qquad S_\pm = \sum_m \ell_m^\pm X_{m\pm1}^m. \tag{4}$$

In general, $f(S_z) = \sum_m f(m) X_m^m$ for any operator function $f(S_z)$; this gives the second-order 'moments': $S_z^2 = \sum_m m^2 X_m^m$ and $S_x^2 + S_y^2 = \sum_m [S(S+1) - m^2] X_m^m$.

Concerning dynamics, the evolution in the *Heisenberg* representation of an operator is governed by $i(dA/dt) = [A, \mathcal{H}]$. This plus Hamiltonian (1) gives for X_n^m

$$\frac{d}{dt} X_n^m = i\Delta_{nm} X_n^m + \frac{i}{2} B_+ \left(\ell_m^+ X_n^{m+1} - \ell_n^- X_{n-1}^m \right) + \frac{i}{2} B_- \left(\ell_m^- X_n^{m-1} - \ell_n^+ X_{n+1}^m \right) \tag{5}$$

(see appendix C) where Δ_{nm} is the frequency associated with the $m \to n$ transition

$$\Delta_{nm} \equiv \varepsilon_n - \varepsilon_m, \qquad \varepsilon_m = -Dm^2 - B_z m, \tag{6}$$

---

[1] Hamiltonian (1) also describes a set of N two-level systems interacting uniformly (Lipkin–Meshkov–Glick model) [34]. The spectrum of 2^N eigenvalues splits into multiplets characterized by a certain $S \leqslant N/2$ and described by a pseudo-spin Hamiltonian $\mathcal{H} = -DS_z^2 - B_x S_x$; the excitation energy of each two-level element corresponds to the field and their coupling to the anisotropy parameter. This is a problem where the feasibility of handling large values of S (large N) is important.

between levels of the diagonal part of the Hamiltonian. In the absence of transverse fields the evolution is simply $X_n^m(t) = e^{i(t-t_0)\Delta_{nm}}X_n^m(t_0)$. In general, $B_{\pm} = B_x \pm iB_y$ couples the dynamics of the diagonal elements, X_m^m, with the adjacent sub-diagonals, $X_m^{m\pm1}$ and $X_{m\pm1}^m$, and so on.

Finally, the density operator is expressed as $\varrho = \sum_{nm}\varrho_{nm}X_n^m$. The quantum-statistical average of X_n^m then follows from the trace formula $\langle A \rangle = \text{Tr}(\varrho A)$ and reads $\langle X_n^m \rangle = \varrho_{mn}$ (appendix C). This is important as it enables working with the density-matrix elements $\varrho_{nm} = \langle n|\varrho|m\rangle$ or the X_n^m interchangeably, since all the equations we are going to handle are linear in X and their averaging thus trivial.

3. Spin weakly coupled to a bosonic bath (dissipative dynamics)

We address now the dynamics of the spin taking into account the coupling to its surroundings. Let us consider a total Hamiltonian including that of the spin $\mathcal{H}(\boldsymbol{S})$, a bath of bosons $\mathcal{H}_b = \sum_q \omega_q a_q^+ a_q$, and their interaction

$$\mathcal{H}_{\text{tot}} = \mathcal{H}(\boldsymbol{S}) + \sum_q c_q F_q(\boldsymbol{S})\left(a_q^+ + a_{-q}\right) + \mathcal{H}_b. \tag{7}$$

Here c_q are coupling constants. The spin-dependent part of the interaction $F_q(\boldsymbol{S})$ is typically a low-degree polynomial of $\boldsymbol{S}$ [28, 36]. The coupling written is linear in the bath operators—only 1-boson processes are included, no Raman scattering involving two quanta (for interactions non-linear in the bath variables, see [24, 31, 37]). Note that no counterterms are included in $\mathcal{H}_{\text{tot}}$ to compensate for the coupling-induced renormalization of the spin levels [6]; we will address this point below.

The total spin-plus-bath system is unlikely to be in a pure state and a density-matrix description is required. For observables depending only on the spin, the required object is the *reduced* density operator $\varrho = \text{Tr}_b(\varrho_{\text{tot}})$, where one traces the bath out. For *weak* system–bath coupling a closed dynamical equation for ϱ can be obtained by perturbation theory. This is the case of many problems in quantum optics, chemical physics or magnetism [1, 3]. The equation has the generic form $i(d\varrho/dt) = [\mathcal{H}, \varrho] + iR[\varrho(\tau)]$, where the *relaxation term R* adds to the Von Neuman evolution the effects of the bath.

In the Hubbard framework, the Heisenberg time evolution of $X_n^m = |n\rangle\langle m|$ is governed by an analogous equation [31, 32]

$$dX_n^m/dt = -i[X_n^m, \mathcal{H}] + R_n^m. \tag{8}$$

The commutator generates the isolated-spin unitary evolution (equation (5)) and R_n^m accounts for the dissipation. When $F(\boldsymbol{S})$ does not depend on the boson index (this is transferable to c_q; see equation (7)), the relaxation term can be written as

$$R_n^m = -\int_{-\infty}^t d\tau\left\{\mathcal{K}(\tau - t)F(\tau)[F, X_n^m] - \mathcal{K}(t - \tau)[F, X_n^m]F(\tau)\right\}. \tag{9}$$

This form is equivalent to the standard dissipative terms for ϱ obtained by projection operators or cumulant expansions to second order [3, appendix 1.A]. The *memory kernel* is the autocorrelation $\mathcal{K}(\tau) \equiv \langle E(t+\tau)E(t)\rangle_b$ of the bath operator $E = \sum_q c_q(a_q^+ + a_{-q})$, and reads $\mathcal{K}(\tau) = \sum_q |c_q|^2[n_q e^{+i\omega_q\tau} + (n_q+1)e^{-i\omega_q\tau}]$, with $n_q = 1/(e^{\omega_q/T} - 1)$ boson occupation numbers. This is how the temperature enters in the formalism, as the bath is assumed in equilibrium at the initial time $\tau \to -\infty$. The operators without argument in equation (9) are evaluated at t whereas $F(\tau) = \sum_{kl} F_{kl}X_k^l(\tau)$ introduces formally the previous history of the spin (cf next section).

It is convenient to introduce the (coupling weighted) *spectral density* of bath modes $J(\omega) = \sum_q |c_q|^2 \pi \delta(\omega - \omega_q)$. All quantities incorporating environmental effects can be expressed in terms of $J(\omega)$. For instance, the kernel $\mathcal{K}(\tau)$ is given by

$$\mathcal{K}(\tau) = \int_0^\infty \frac{d\omega}{\pi} J(\omega) \left[n_\omega \, e^{+i\omega\tau} + (n_\omega + 1) \, e^{-i\omega\tau} \right], \tag{10}$$

with $n_\omega = 1/(e^{\omega/T} - 1)$. A common functional form for the spectral density is $J(\omega) \propto \omega^\alpha$ (times a high-frequency cut-off at ω_D). The bath is called *Ohmic* when $\alpha = 1$; this is realized by the Kondo coupling to electron–hole pairs near the Fermi energy in solids (an example of bosonizable excitations from the ground state of a non-bosonic environment [6]). For $\alpha > 1$ the bath is called *super-Ohmic*; for instance, interaction with photons or phonons in three dimensions gives $J(\omega) \propto \omega^3$ [1].

We shall write $J(\omega) = \lambda \omega^\alpha$ with λ, determined by the $|c_q|^2$, an overall measure of the coupling strength (classically, the damping parameter). The characteristic 'width' of the memory kernel, τ_b, depends on the competition of $1/T$ and $1/\omega_D$, the bath bandwidth (Debye frequency for phonons). The relaxation term (9) was obtained treating the coupling perturbatively to the second order for small $\lambda \tau_b$.

4. Markovian (time-local) density-matrix equations

Due to the integral term (9) the master equation is formally an integro-differential equation for X_n^m. To second order in the coupling, however, the retarded dependences $F(\tau) = \sum_{kl} F_{kl} X_k^l(\tau)$ can be replaced by their unitary evolution, $F(\tau) = U(\tau - t)F(t)$. Introducing these time dependences in R only operators evaluated at t do remain.

To illustrate, let us assume the Hamiltonian evolution simply given by $X_k^l(\tau) = e^{i(\tau - t)\Delta_{kl}} X_k^l(t)$. This can be plugged in R_n^m and the resulting operator combinations $X_k^l \left[F, X_n^m \right]$ are expressed in the Hubbard basis and simplified using $X_n^m X_k^l = \delta_{mk} X_n^l$. This results in an equation of motion fully in terms of $X_n^m(t)$, and *linear* in them. Carrying out these steps one actually gets the relaxation term (appendix D.1)

$$R_n^m = \sum_{n'm'} \left[-\delta_{mm'} \sum_\ell W_{\ell|n'}^* F_{n'\ell} F_{\ell n} \right.$$
$$+ (W_{n|n'}^* + W_{m|m'}) F_{n'n} F_{mm'}$$
$$\left. - \delta_{nn'} \sum_\ell W_{\ell|m'} F_{m\ell} F_{\ell m'} \right] X_{n'}^{m'}. \tag{11}$$

The coefficients include the matrix elements of the spin portion of the coupling, $F_{nm} = \langle n|F(\boldsymbol{S})|m \rangle$, and the $m \to n$ (complex) transition rates

$$W_{n|m} \equiv W(\Delta_{nm}), \qquad W(\Delta) = \int_0^\infty d\tau \, e^{-i\tau\Delta} \mathcal{K}(\tau), \tag{12}$$

evaluated at the level differences $\Delta_{nm} = \varepsilon_n - \varepsilon_m$. The form of the rate function $W(\Delta)$ emerges directly from the retarded dependences $X(\tau) = e^{-i(t-\tau)\Delta} X(t)$, which yield oscillating factors $e^{-i\tau\Delta}$ multiplying the kernel $\mathcal{K}(\tau)$ in the integrand of equation (9). On the other hand, the quantum-statistical average of the above R_n^m, using $\langle X_n^m \rangle = \varrho_{mn}$, gives an equation for the matrix elements $\langle n|\varrho|m \rangle$ which coincides with what can be obtained from the standard, second-order, relaxation terms for ϱ [3, appendix 1.A].

Let us discuss when the conservative evolution of $X_k^l(\tau)$ can be substituted by $e^{i(\tau - t)\Delta_{kl}} X_k^l(t)$ in our problem. If one uses the basis of eigenstates of the full spin Hamiltonian (including the transverse terms [38, 39]), such evolution is *exact* (then $B_\pm$ do not appear

explicitly in the equation of motion, but only via Δ_{nm} appendix C). Further, if the transverse field is not too large, one can use the angular-momentum basis; then $X_n^m(\tau) \simeq e^{i(\tau-t)\Delta_{nm}} X_n^m(t)$ gives the dominant Hamiltonian dependences, providing an *approximate* relaxation term[2]. This way of getting a time-local relaxation, without resorting to $T \to \infty$ approximations or semiclassical baths [6], works when one explicitly knows the conservative evolution; apart from simple spin problems, it also applies to the harmonic oscillator [40, 41].

4.1. Relaxation term for couplings via $S_\pm$

In various important cases the coupling is realized through $S_\pm = S_x \pm iS_y$. For instance, $F \sim S_\pm$ appears in the Kondo coupling to electron–hole excitations and $F \sim \{S_z, S_\pm\}$ in magnetoelastic interaction with phonons [29, 32]. Thus we will consider the form

$$F(\boldsymbol{S}) = \eta_+ \{v(S_z), S_-\} + \eta_- \{v(S_z), S_+\}, \tag{13}$$

where $\{A, B\} = AB + BA$ and $\eta_\pm = \eta_x \pm i\eta_y$ are scalars incorporating the symmetry of the interaction (isotropic $\eta_x = \eta_y = 1$; anisotropic $\eta_x = 1$ and $\eta_y = 0$, etc). The matrix elements $F_{nm} = \langle n|F|m \rangle$ are then (appendix D.2)

$$F_{nm} = L_{m,m-1}\delta_{n,m-1} + L_{m+1,m}^* \delta_{n,m+1}, \qquad L_{m,m'} = \eta_+[v(m) + v(m')]\ell_{m,m'}, \tag{14}$$

where $L_{m,m'}$ is an extended ladder factor with $\ell_{m,m\pm1} = [S(S+1) - m(m \pm 1)]^{1/2} = \ell_m^\pm$. Although the operator $v(S_z)$ commutes with S_z, it modulates via $[v(m) + v(m')]$ the matrix elements of $S_\pm$, which are ultimately responsible for transitions between the levels $|m\rangle$. The inclusion of a $\eta_z S_z$ term in F does not lead to structurally new terms in the final equation and will not be considered here (it produces 'dephasing' but not dissipation [3, chapter 10]; in the language of magnetic resonance it modifies T_2).

The particularization of the relaxation term (11) to the coupling (13) is done in appendix D.2. Invoking on it the *secular* approximation one is left with

$$\begin{aligned}
R_n^m = {} & L_{n,n-1}L_{m,m-1}^*(W_{n|n-1}^* + W_{m|m-1})X_{n-1}^{m-1} \\
& - (|L_{n,n+1}|^2 W_{n+1|n}^* + |L_{m,m+1}|^2 W_{m+1|m} \\
& + |L_{n,n-1}|^2 W_{n-1|n}^* + |L_{m,m-1}|^2 W_{m-1|m})X_n^m \\
& + L_{n,n+1}^* L_{m,m+1}(W_{n|n+1}^* + W_{m|m+1})X_{n+1}^{m+1}.
\end{aligned} \tag{15}$$

This corresponds to the *rotating-wave* approximation familiar in quantum optics, where counterrotating, rapidly oscillating terms, are averaged out (appendix D.3). Such manipulations do not seem to pose problems for a very weak coupling, while they simplify the treatment [42, 43]. In addition, the illustration of the continued-fraction approach will be cleaner disregarding non-secular terms in the master equation.

To conclude, it is argued that the imaginary parts of the relaxation coefficients reflect a coupling-induced renormalization of the levels, not genuine relaxation. In the bath-of-oscillators formalism this renormalization is cancelled out by including suitable 'counterterms' in the starting system-plus-bath Hamiltonian [6]. In the spin case Garanin *et al* [31, 32] cancel them by omitting the imaginary parts of $W_{n|m}$, redefining $W(\Delta) \equiv \text{Re}\left[\int_0^\infty d\tau\, e^{-i\tau\Delta}\mathcal{K}(\tau)\right]$.[3]

---

[2] Classically, such R_n^m corresponds to using $\boldsymbol{R} = -\lambda_{\text{LL}}\boldsymbol{S} \times (\boldsymbol{S} \times z B_{\text{eff}}^z)$ as relaxation term in the Landau–Lifshitz equation, fully keeping the Hamiltonian precession $d\boldsymbol{S}/dt = (\boldsymbol{S} \times \boldsymbol{B}_{\text{eff}}) + \boldsymbol{R}$. (Here $\boldsymbol{B}_{\text{eff}} = -\partial\mathcal{H}/\partial\boldsymbol{S}$; the form $\boldsymbol{S} \times \partial\mathcal{H}/\partial\boldsymbol{S}$ follows from $dS_i/dt = \{S_i, \mathcal{H}\}$ via the Poisson brackets $\{S_i, S_j\} = \epsilon_{ijk}S_k$ [34]). The z-component of B_{eff} retained in $\boldsymbol{R}$ incorporates the anisotropy field $B_a \sim 2DS$, the dominant energy scale in superparamagnets.

[3] The formalism assumes that it was previously assessed whether such a renormalization is physically meaningful for a given coupling, and if so (e.g., the Lamb shift), it is considered to be already included in $\mathcal{H}(\boldsymbol{S})$. This has the advantage of making $\mathcal{H}$ the experimentally accessible Hamiltonian, instead of the bare one which may be difficult to determine.

4.2. Elements and structure of the resulting density-matrix equation

The basic ingredients of the master equation are the energy differences Δ_{nm}, transverse fields $B_\pm$, ladder factors, coupling matrix elements $\langle n|F|m\rangle \sim L_{m,m'}$ and transition rates $W_{n|m} = W(\Delta_{nm})$. All properties of the bath enter via the rate function, which can be expressed in terms of the spectral density $J(\omega)$ as follows (appendix E)

$$W(\Delta > 0) = J(\Delta)n_\Delta, \qquad W(\Delta < 0) = J(|\Delta|)(n_{|\Delta|} + 1). \qquad (16)$$

As $n_\omega = 1/(e^{\omega/T} - 1)$ boson absorption and emission rates are related by the *detailed balance* condition $W(\Delta) = e^{-\Delta/T}W(-\Delta)$. This ensures, under certain conditions, convergence to the Gibbs distribution at long times [42, 43].

The rates in the relaxation term (15) involve adjacent levels only, $W_{m|m\pm1} = W(\Delta_{m,m\pm1})$, while R_n^m connects X_n^m with X_k^l differing in indices by at most 1. Thus in the following we will compactly write

$$R_n^m = \mathcal{W}_{n,n-1}^{m,m-1} X_{n-1}^{m-1} + \mathcal{W}_{n,n}^{m,m} X_n^m + \mathcal{W}_{n,n+1}^{m,m+1} X_{n+1}^{m+1}, \qquad (17)$$

which together with equations (5) and (8) gives the working equation

$$\dot{X}_n^m = \mathrm{i}\Delta_{nm}X_n^m + \tfrac{\mathrm{i}}{2}B_+\left(\ell_m^+ X_n^{m+1} - \ell_n^- X_{n-1}^m\right) + \tfrac{\mathrm{i}}{2}B_-\left(\ell_m^- X_n^{m-1} - \ell_n^+ X_{n+1}^m\right)$$
$$+ \mathcal{W}_{n,n-1}^{m,m-1} X_{n-1}^{m-1} + \mathcal{W}_{n,n}^{m,m} X_n^m + \mathcal{W}_{n,n+1}^{m,m+1} X_{n+1}^{m+1}. \qquad (18)$$

It is worth mentioning that the density-matrix equation was obtained within a, though approximate, fully quantum treatment, not introducing any phenomenological relaxation or assuming preconceived structures for the equation.

Note finally that if the transverse field is set to zero, $B_\pm = 0$, the diagonal part of equation (18) becomes a closed system of *balance equations* for the level 'populations' $N_m \equiv X_m^m$, as in the Pauli master equation approach

$$\dot{N}_m = \mathcal{W}_m^- N_{m-1} + \mathcal{W}_m N_m + \mathcal{W}_m^+ N_{m+1}. \qquad (19)$$

As $\Delta_{mm} = 0$, the Hamiltonian part does not show up and the dynamics is purely relaxational $\left(\mathcal{W}_m^- = \mathcal{W}_{m,m-1}^{m,m-1}, \mathcal{W}_m = \mathcal{W}_{m,m}^{m,m}, \mathcal{W}_m^+ = \mathcal{W}_{m,m+1}^{m,m+1}\right)$. For example, in the case of an isotropic spin in a *static* field we can always choose the z-axis so that $\mathcal{H} = -B_z S_z$. However, if we want to study resonance phenomena, we need the full equation (18) to account for transverse probing fields. Further, even if $B_\pm \equiv 0$ (or when using exact eigenstates of the full Hamiltonian), the simple balance structure (19) is broken by terms like X_{m-1}^{m+1} or X_m^{m-2} if not resorting to the secular approximation (appendix D.2). For these reasons we will focus on full density-matrix equations.

5. Density-matrix equations for specific spin–bath problems

Here we particularize equation (18) to an isotropic spin with truly linear coupling $F \sim S_\pm$, as that to electron–hole excitations (an Ohmic bath), and to anisotropic spins with $F \sim \{S_z, S_\pm\}$, corresponding to interaction with phonons (a bath from Ohmic to super-Ohmic depending on the lattice dimensionality). In the classical limit, the first coupling yields *field-type* fluctuations in the spin Langevin equations [25, 26], whereas the second produces *anisotropy-type* fluctuations [24, 44, 45] (the spin analogue of force-type and frequency-type fluctuations in mechanical systems [46]).

5.1. Density-matrix equation for isotropic spins

Let us consider a spin $\mathcal{H} = -\boldsymbol{B} \cdot \boldsymbol{S}$, with the linear coupling $F = \frac{1}{2}(\eta_+ S_- + \eta_- S_+)$. This corresponds to a constant $v(S_z) = 1/4$ in equation (13). Then $L_{m,m'} = \frac{1}{2}\eta_+ \ell_{m,m'}$ in the matrix elements F_{nm} and hence $L_{n,n'}L_{m,m'}^* = \frac{1}{4}|\eta|^2 \ell_{n,n'}\ell_{m,m'}$, with $|\eta|^2 = \eta_+\eta_-$. On the other hand, as the transition rates involve adjacent levels $W_{m|m\pm1} = W(\Delta_{m,m\pm1})$, and here $\Delta_{m,m\pm1} = \pm B_z$, only two rates appear. Introducing $w_0 \equiv W_{m|m-1}$ for the $m-1 \to m$ transition (decay for $B_z > 0$), and $W_{m-1|m} = w_0\, \mathrm{e}^{-B_z/T}$ by detailed balance, the relaxation term (15) reduces to

$$R_n^m = w_0\big\{\ell_{n-1}\ell_{m-1}X_{n-1}^{m-1} - \tfrac{1}{2}\big[(\ell_n^2 + \ell_m^2) + \mathrm{e}^{-y}(\ell_{n-1}^2 + \ell_{m-1}^2)\big]X_n^m + \mathrm{e}^{-y}\ell_n\ell_m X_{n+1}^{m+1}\big\}. \tag{20}$$

Here we have introduced $y = B_z/T$, the single factor $\ell_m = [S(S+1) - m(m+1)]^{1/2}$ (then $\ell_m^+ = \ell_m$ and $\ell_m^- = \ell_{m-1}$), and assumed isotropic coupling $\eta_x = \eta_y = 1$ ($|\eta|^2$ simply rescales w_0). Using this relaxation term and the Zeeman transition frequency $\Delta_{nm} = -B_z(n-m)$ in the master equation (18), one finally gets

$$\dot{X}_n^m = -\mathrm{i}B_z(n-m)X_n^m + \tfrac{\mathrm{i}}{2}B_+\big(\ell_m X_n^{m+1} - \ell_{n-1}X_{n-1}^m\big) + \tfrac{\mathrm{i}}{2}B_-\big(\ell_{m-1}X_n^{m-1} - \ell_n X_{n+1}^m\big)$$
$$+ w_0\big\{\ell_{n-1}\ell_{m-1}X_{n-1}^{m-1} - \tfrac{1}{2}\big[(\ell_n^2 + \ell_m^2) + \mathrm{e}^{-y}(\ell_{n-1}^2 + \ell_{m-1}^2)\big]X_n^m + \mathrm{e}^{-y}\ell_n\ell_m X_{n+1}^{m+1}\big\}. \tag{21}$$

This equation corresponds to the master equation of Garanin [31] (he also included 2-boson Raman processes). For $B_\pm = 0$ the diagonal elements obey the balance equations (19) with $\mathcal{W}_m^- = w_0\ell_{m-1}^2$, $\mathcal{W}_m = -w_0(\ell_m^2 + \mathrm{e}^{-y}\ell_{m-1}^2)$ and $\mathcal{W}_m^+ = w_0\mathrm{e}^{-y}\ell_m^2$.

In an Ohmic bath $J(\omega) = \lambda\omega$ the rate function is $W(\Delta) = \lambda\Delta/(\mathrm{e}^{\Delta/T} - 1)$ (this form is valid for both signs of Δ; see appendix E). Then $w_0 = \lambda T y/(1 - \mathrm{e}^{-y})$ which in the limit $y \to 0$ goes over the classical rotational-diffusion constant $w_0 \to \lambda T$ (independent of B_z); thus λ from $J(\omega)$ plays the role of the Landau–Lifshitz damping parameter. Actually, taking the limit $S \to \infty$ in the balance equations [47, appendix A] one gets the classical Fokker–Planck equation (in a longitudinal field), and the correspondence is established as $2\lambda S \to \lambda_{\mathrm{LL}}$.

5.2. Density-matrix equation for superparamagnets

Next we consider anisotropic spins, $\mathcal{H} = -DS_z^2 - \boldsymbol{B} \cdot \boldsymbol{S}$, with a coupling linear in $S_\pm$ but with S_z-dependent 'coefficients', as it occurs in spin–lattice interactions. There $F = \frac{1}{2}\{S_z, \eta_+ S_- + \eta_- S_+\}$, corresponding to $v(S_z) = S_z/2$ in equation (13). For $|\eta|^2 = 2$ this gives $L_{n,n'}L_{m,m'}^* = \frac{1}{2}\bar{\ell}_{n,n'}\bar{\ell}_{m,m'}$, with the modulated factors $\bar{\ell}_{m,m'} = (m+m')\ell_{m,m'}$. Then the density-matrix equation (18) goes over

$$\dot{X}_n^m = \mathrm{i}\Delta_{nm}X_n^m + \tfrac{\mathrm{i}}{2}B_+\big(\ell_m X_n^{m+1} - \ell_{n-1}X_{n-1}^m\big) + \tfrac{\mathrm{i}}{2}B_-\big(\ell_{m-1}X_n^{m-1} - \ell_n X_{n+1}^m\big)$$
$$+ \tfrac{1}{2}\bar{\ell}_{n-1}\bar{\ell}_{m-1}(W_{n|n-1} + W_{m|m-1})X_{n-1}^{m-1} + \tfrac{1}{2}\bar{\ell}_n\bar{\ell}_m(W_{n|n+1} + W_{m|m+1})X_{n+1}^{m+1}$$
$$- \tfrac{1}{2}\big(\bar{\ell}_n^2 W_{n+1|n} + \bar{\ell}_m^2 W_{m+1|m} + \bar{\ell}_{n-1}^2 W_{n-1|n} + \bar{\ell}_{m-1}^2 W_{m-1|m}\big)X_n^m, \tag{22}$$

where $\Delta_{nm} = -[D(n+m) + B_z](n-m)$ and we have introduced the corresponding 1-index notation $\bar{\ell}_m = (2m+1)\ell_m$ (appendix B). This equation was derived in [32] for the study of the archetypal magnetic molecular cluster Mn$_{12}$. The replacement $\ell_m \to \bar{\ell}_m$ (not affecting the Hamiltonian part) accounts for the S_z-dependent coupling and results in an extra m dependence of the relaxation term with respect to the case $F \sim S_\pm$. It can be seen as a level-dependent 'damping' $\lambda_{\mathrm{eff}}(m) \sim \lambda(2m+1)^2$, decreasing as the anisotropy barrier $m \sim 0$ is approached (figure 14); a spin analogue of position-dependent damping in translational Brownian motion.

Rates $W_{n|m}$ involve adjacent levels but no simplification arises here due to the non-equispaced spectrum of anisotropic spins $\Delta_{m,m\pm1} = \pm[D(2m \pm 1) + B_z]$. To get the rate function $W(\Delta)$ one can compute the distribution of bath excitations $J(\omega) = \sum_q |c_q|^2\pi\delta(\omega - \omega_q)$ with a Debye phonon model $\omega_{ks} = v_s|k|$ and replace $\sum_q \to \sum_s \int\mathrm{d}^d\boldsymbol{k}$, integrating over

wave-vectors and summing over branches. For a magnetoelastic coupling one has $|c_q|^2 \sim \omega_q$ so that $\mathrm{d}^d k \times |c_{ks}|^2 \sim |k|^{d-1} \times |k|$ gives spectral densities $J \propto \omega^\alpha$ evolving from Ohmic $\alpha = 1$, for phonons in one dimension, to super-Ohmic $J \propto \omega^3$ for $d = 3$. The corresponding relaxation functions are

$$W(\Delta) = \lambda \Delta^\alpha / (\mathrm{e}^{\Delta/T} - 1), \qquad \forall \Delta. \tag{23}$$

This unified form, instead of equation (16), is discussed in appendix E. Note that phonon velocities v_s, coupling constants, etc, are subsumed in λ from $J(\omega) = \lambda \omega^\alpha$.

6. Response to probing fields: perturbative density-matrix equations

With the master equations one can describe the non-equilibrium evolution from one stationary state to another. A system can be made to 'relax' either by subjecting it to a 'force' (a magnetic, electric, stress field, etc) or by removing it after having kept it for a long time. Then the question is how the infusion or withdrawal of energy is shared by the system's degrees of freedom. Alternatively one can apply a force oscillating with frequency Ω; this provides a time scale $1/\Omega$ whose competition with the intrinsic scales of the system permits us to analyse its different dynamical modes [48].

To reflect intrinsic properties the probe should be suitably small, not altering the nature of the studied system. This has the advantage of allowing the use of perturbation theory in the treatment. In this section, we will replace B by $B + \delta B$ in the spin density-matrix equation, and treat it perturbatively in δB, getting a chain of coupled equations. Each level will be tackled sequentially with the continued-fraction treatment of section 7, giving the spin response to the perturbation (susceptibilities).

To alleviate the notation, we first write the density-matrix equation (18) in the following compact form (including all n and m)

$$\dot{X} = \mathrm{i}\Delta(B)X + \mathcal{W}(B)X. \tag{24}$$

Here $\mathrm{i}\Delta X$ stands for *all* the Hamiltonian part (we put the 'i' to remind us of this) and $\mathcal{W}X$ for the relaxation term. The field enters via $\mathrm{i}\Delta$ linearly (equation (5)) and non-linearly through $\Delta_{m,m\pm1} = \pm[D(2m \pm 1) + B_z]$ in the rates $W(\Delta) \sim \Delta^\alpha n_\Delta$. Let us now augment B by a probing field, $B \to B + b(t)u$, with $u = (u_x, u_y, u_z)$ a unit vector along δB and $b(t) = b\cos(\Omega t)$ its magnitude. To obtain *linear* susceptibilities, we expand field-dependent parameters $f = f(B_x, B_y, B_x)$ to first order: $f \simeq f_0 + f_1 b(t)$, with $f_\kappa = (\mathrm{d}^\kappa f/\mathrm{d}b^\kappa)/\kappa!$ derivatives with respect to the *amplitude* $\mathrm{d}/\mathrm{d}b = \sum_i u_i \partial_{B_i}$. For the coefficients of the master equation this gives $\mathrm{i}\Delta = \mathrm{i}\Delta_0 + \mathrm{i}\Delta_1 b(t)$ and $\mathcal{W} \simeq \mathcal{W}_0 + \mathcal{W}_1 b(t)$ (the former is exact as Δ is linear in B).

Although modulated quantities like $\mathrm{i}\Delta$ and $\mathcal{W}$ have the parametric time dependence $f(t) = f[B + b(t)]$ (appendix D.3), our dynamical variable $X(t)$ does not need to evolve as some function of $B + b(t)$. Thus, we seek for a solution of the form (no (t) in b)

$$X(t) \simeq X_0(t) + X_1(t)b. \tag{25}$$

We compute now $\mathrm{i}\Delta \times X$ and $\mathcal{W} \times X$ to the first order, replace them in the dynamical equation (24), and equate terms with the same power of b, getting ($X_{-1} \equiv 0$)

$$\dot{X}_\kappa = (\mathrm{i}\Delta_0 + \mathcal{W}_0)X_\kappa + (\mathrm{i}\Delta_1 + \mathcal{W}_1)\cos(\Omega t)X_{\kappa-1}. \tag{26}$$

The perturbative structure is clear: the original equation with unperturbed coefficients (first term) plus their derivatives $(\cdot)_1$ times the previous-order result. Thus the lower level $X_{\kappa-1}$ acts as a forcing (source) term when solving the equation for X_κ.

To get the long-time *stationary response*, when all transients have died out, we introduce Fourier expansions (subindex for order in b, superindex for the harmonic)

$$\boldsymbol{X}_\kappa(t) = \frac{1}{2^\kappa} \sum_\nu \boldsymbol{X}_\kappa^{(\nu)} \, \mathrm{e}^{\nu \mathrm{i}\Omega t}, \tag{27}$$

and go order by order. The harmonics $\mathrm{e}^{\nu \mathrm{i}\Omega t}$ generated at each κ will coincide with those of the forcing $\cos(\Omega t)\boldsymbol{X}_{\kappa-1}(t)$, because equation (26) is linear in $\boldsymbol{X}_\kappa$ *and* $\boldsymbol{X}_\kappa$ itself is not multiplied by oscillating terms (additive sources). The *zeroth*-order equation $\dot{\boldsymbol{X}}_0 = (\mathrm{i}\Delta_0 + \mathcal{W}_0)\boldsymbol{X}_0$ has no sources. Then, only $\nu = 0$ is left in the Fourier series, $\boldsymbol{X}_0 = \boldsymbol{X}_0^{(0)}$, and the static response obeys $0 = (\mathrm{i}\Delta_0 + \mathcal{W}_0)\boldsymbol{X}_0^{(0)}$. At the *first* order the forcing is $\cos(\Omega t)\boldsymbol{X}_0 = \frac{1}{2}(\mathrm{e}^{+\mathrm{i}\Omega t} + \mathrm{e}^{-\mathrm{i}\Omega t})\boldsymbol{X}_0^{(0)}$ and only the harmonics $\nu = \pm 1$ get excited ($\boldsymbol{X}_1^{(0)} \equiv 0$). Thus we use $\boldsymbol{X}_1 = \frac{1}{2}\left(\boldsymbol{X}_1^{(1)}\mathrm{e}^{+\mathrm{i}\Omega t} + \boldsymbol{X}_1^{(-1)}\mathrm{e}^{-\mathrm{i}\Omega t}\right)$ in equation (26) and equate Fourier coefficients on both sides, getting the remaining equations

$$\begin{cases} 0 = (\mathrm{i}\Delta_0 + \mathcal{W}_0)\boldsymbol{X}_0^{(0)} + 0 \\ \pm \mathrm{i}\Omega \boldsymbol{X}_1^{(\pm 1)} = (\mathrm{i}\Delta_0 + \mathcal{W}_0)\boldsymbol{X}_1^{(\pm 1)} + \left(\mathrm{i}\Delta_1 + \mathcal{W}_1\right)\boldsymbol{X}_0^{(0)}. \end{cases} \tag{28}$$

These equations are to be solved sequentially by the continued-fraction method, with the previous order acting as a forcing on the next.

Some final remarks. Technically, we use an *equation-of-motion* approach to obtain the response, not relying on Kubo-type linear-response-theory expressions [48]. This allows proceeding systematically to higher orders to get *non-linear susceptibilities* (harmonics of the excitation generated by non-linearities). Then, one finds terms of the form $\sum_{l \geqslant 2}^\kappa \mathcal{W}_l \cos^l(\Omega t)\boldsymbol{X}_{\kappa-l}$ in the equation for $\boldsymbol{X}_\kappa$, due to the non-linearity of the relaxation term (which includes $W(\Delta) = \lambda\Delta^\alpha/(\mathrm{e}^{\Delta/T} - 1)$). In quantum Brownian motion as described by the Caldeira–Leggett equation [6, 21], due to the high-T approximations plus Ohmic bath (corresponding to $W \simeq \lambda T$), the relaxation term does not depend on the system potential: $R = -\mathrm{i}\gamma\left[\frac{1}{2}(x-y)(\partial_x - \partial_y) + T(x-y)^2\right]\varrho(x, y)$ or $R = \gamma\partial_p(p + T\partial_p)W(x, p)$ in the Wigner representation. In particular, R does not depend on the forcing, and such higher derivative terms vanish ($\mathcal{W}_{l \geqslant 2} \equiv 0$). They are also absent in classical spins and dipoles [49, 50], where the relaxation term *does* depend on the field, $\boldsymbol{R} = -\lambda_{\mathrm{LL}}\boldsymbol{S} \times (\boldsymbol{S} \times \boldsymbol{B}_{\mathrm{eff}})$, but linearly. Anyway, as we have seen, the $\mathcal{W}_{l \geqslant 2}$ terms do not affect the calculation of the linear responses.

7. Continued-fraction methods for spin density-matrix equations

To solve the master equations we will cast them into the form of 3-term recurrence relations suitable to apply the continued-fraction method [4]. This is related to the schemes of solution by tri-diagonalization, like the Lanczos algorithm or the recursion method [51]. In Brownian motion problems it shares elements with the expansion into complete sets (Grad's) approach for solving kinetic equations [5]. The non-equilibrium distribution W is expanded in a basis of functions (Hermite or Laguerre polynomials, plane waves, spherical harmonics, etc) and the partial-differential kinetic equation is transformed into a *set of coupled equations* for the expansion coefficients C_i. Approximate solutions can be obtained by truncating the hierarchy of equations at various levels. But as a matter of fact, to obtain manageable equations the truncation needs to be performed at a low level. In the continued-fraction variant, instead of truncating directly, one seeks for bases in which the range of index coupling is short (ideally, the equation for C_i involves C_{i-1}, C_i and C_{i+1}). Then these recurrences between C_i can be solved exactly by iterating a simple algorithm, which has the structure of a continued-fraction[4].

---

[4] For a nice brief survey of the relation between ordinary series expansions, orthogonal polynomials, recursions and continued fractions, see [52].

This technique was exploited to solve classical Fokker–Planck equations for few-variable systems in external potentials [14–16]. Compared with direct simulations, continued-fraction methods have several *shortcomings*: (i) the basis choice is quite problem specific, (ii) the stability and convergence of the algorithm may fail in some ranges of parameters, and (iii) it does not return trajectories (which always provide helpful insight). When the method works, however, its *advantages* are valuable: (i) no statistical errors, (ii) special aptness to get stationary solutions (long times), (iii) high efficiency, allowing us to explore parameter ranges out of reach of simulation, and (iv) the obtaining of the distribution W (also insightful).

This, together with the lack of quantum Langevin simulations, motivated several adaptations of the continued-fraction approach to quantum problems [18–20]. The master equation was transformed into Fokker–Planck-like form using pseudo-probability representations W of the density matrix, then such W was expanded in appropriate bases and the recurrences for the coefficients were derived from the kinetic equation and solved by continued fractions. As this approach is not based on the Hamiltonian eigenstructure, it is invaluable for systems including continuous parts in the spectrum (e.g., Morse and periodic potentials). Notwithstanding this, for systems with discrete levels only, the density-matrix equation for ϱ_{nm} already has an index-recurrence structure and such transformation–expansion protocol (often cumbersome) may be bypassed. This is our purpose in this section (cf [53, 54, section V] for $S = 1/2$).

7.1. Index-coupling structure and vector 3-term recurrences

Let us begin writing the master equation (18) compactly as $\dot{X}_n^m = \sum_{n'm'} Q_{n,n'}^{m,m'} X_{n'}^{m'}$, with $n' = n - 1, n, n + 1$ and $m' = m - 1, m, m + 1$, and with coefficients

$$
\begin{aligned}
&Q_{n,n-1}^{m,m-1} = \mathcal{W}_{n,n-1}^{m,m-1} & &Q_{n,n-1}^{m,m} = -(\mathrm{i}/2)B_+\ell_n^- & &Q_{n,n-1}^{m,m+1} \equiv 0 \\
&Q_{n,n}^{m,m-1} = (\mathrm{i}/2)B_-\ell_m^- & &Q_{n,n}^{m,m} = \mathrm{i}\Delta_{nm} + \mathcal{W}_{n,n}^{m,m} & &Q_{n,n}^{m,m+1} = (\mathrm{i}/2)B_+\ell_m^+ \qquad (29)\\
&Q_{n,n+1}^{m,m-1} \equiv 0 & &Q_{n,n+1}^{m,m} = -(\mathrm{i}/2)B_-\ell_n^+ & &Q_{n,n+1}^{m,m+1} = \mathcal{W}_{n,n+1}^{m,m+1}.
\end{aligned}
$$

The matrix associated with this linear system has dimensions $(2S + 1)^2 \times (2S + 1)^2$. For small spins it can be solved directly. However, already at $S = 3$ the size is 49×49, becoming 441×441 for $S = 10$ (Mn_{12} or Fe_8), and rising to 1156×1156 for $S = 33/2$ (Fe_{19}) and to 2704×2704 for $S = 51/2$ (Mn_{25}). Thus, if one is tempted to study mesoscopic spins in this way, let alone pursue the classical limit, one soon faces large matrices.

The problem gets simpler if $B_\pm \equiv 0$, as the system splits into uncoupled recurrences inside each sub-diagonal $\dot{X}_m^{m+k} = F\big[X_{m-1}^{(m-1)+k}, X_m^{m+k}, X_{m+1}^{(m+1)+k}\big]$ with fixed k. These can be solved separately by *scalar* continued fractions, as in the approach of Shibata [18]. Nevertheless, in problems involving coherent dynamics the diagonals are typically coupled and such a strategy is not applicable. They remain coupled even when $B_\pm = 0$ (or when using the exact eigenstates of the full Hamiltonian) if not resorting to the rotating-wave approximation (equation (D.3)).

This calls for more generic methods. Our aim is to retain the spirit of Shibata's approach by converting the 2-index recurrence $\dot{X}_n^m = \sum Q_{n,n'}^{m,m'} X_{n'}^{m'}$, into a 1-index *vector* recurrence. To this end, we first rewrite the equations highlighting the index-coupling structure

$$
\begin{aligned}
\dot{X}_n^m = \;&Q_{n,n-1}^{m,m-1} & &X_{n-1}^{m-1} + Q_{n,n}^{m,m-1} & &X_n^{m-1} + 0 & &X_{n+1}^{m-1} \\
+\;&Q_{n,n-1}^{m,m} & &X_{n-1}^{m} + Q_{n,n}^{m,m} & &X_n^{m} + Q_{n,n+1}^{m,m} & &X_{n+1}^{m} \qquad (30)\\
+\;&0 & &X_{n-1}^{m+1} + Q_{n,n}^{m,m+1} & &X_n^{m+1} + Q_{n,n+1}^{m,m+1} & &X_{n+1}^{m+1}.
\end{aligned}
$$

Forgeting for a moment about the upper indices m', we see that the equation for $X_n^{(\cdot)}$ only involves $X_{n-1}^{(\cdot)}$ (first column), $X_n^{(\cdot)}$ itself (second) and $X_{n+1}^{(\cdot)}$ (last). Thus, if we build up 'vectors'

c_n including all X_n^m for a given n we will have a 3-term recurrence between them, with some matrix coefficients $\mathbb{Q}_{n,n'}$. That is, $\dot{c}_n = \mathbb{Q}_{n,n-1}c_{n-1} + \mathbb{Q}_{n,n}c_n + \mathbb{Q}_{n,n+1}c_{n+1}$. This could be tackled by *matrix* continued fractions, replacing the original $(2S+1)^2 \times (2S+1)^2$ problem by one with $2S+1$ steps but with matrices $(2S+1) \times (2S+1)$ (appendix G). This approach actually converts the $\sim S^4$ problem into an overall $\sim S^3$ one and reduces significantly the storage demands. Compared with the previous exact techniques, this will allow us to increase the possible values of S significantly (up to ~ 100–200).

Explicitly, the required $(2S+1)$-tuples c_n and $(2S+1) \times (2S+1)$ matrices $\mathbb{Q}_{n,n'}$ comprise (with averages in $(c_n)_m = \langle X_n^m \rangle$ one deals directly with ϱ_{nm})

$$c_n = \begin{pmatrix} X_n^{-S} \\ \vdots \\ X_n^S \end{pmatrix} \begin{array}{c} \uparrow \\ 2S+1, \\ \downarrow \end{array} \qquad (c_n)_m = X_n^m$$

$$\mathbb{Q}_{n,n'} = \begin{pmatrix} Q_{n,n'}^{-S,\ -S} & Q_{n,n'}^{-S,\ -S+1} & 0 & & & \\ Q_{n,n'}^{-S+1,-S} & Q_{n,n'}^{-S+1,-S+1} & Q_{n,n'}^{-S+1,-S+2} & 0 & & 0 \\ 0 & Q_{n,n'}^{-S+2,-S+1} & Q_{n,n'}^{-S+2,-S+2} & Q_{n,n'}^{-S+2,-S+3} & 0 & \\ & \ddots & \ddots & \ddots & \ddots & \ddots \\ & & 0 & Q_{n,n'}^{m,m-1} & Q_{n,n'}^{m,m} & Q_{n,n'}^{m,m+1} & 0 \\ & 0 & & \ddots & \ddots & \ddots & \ddots \\ & & & & 0 & Q_{n,n'}^{S,S-1} & Q_{n,n'}^{S,S} \end{pmatrix}.$$

$$(31)$$

Then, introducing the custom notation $\mathbb{Q}_n^- \equiv \mathbb{Q}_{n,n-1}$, $\mathbb{Q}_n \equiv \mathbb{Q}_{n,n}$ and $\mathbb{Q}_n^+ \equiv \mathbb{Q}_{n,n+1}$, the density-matrix equation (30) is transformed into the 3-term canonical form:

$$\dot{c}_n = \mathbb{Q}_n^- c_{n-1} + \mathbb{Q}_n c_n + \mathbb{Q}_n^+ c_{n+1}, \qquad n = -S, \ldots, S. \qquad (32)$$

It is worth emphasizing the simple attainment of the sought recursion form in comparison with the Fokker–Planck-like approach with pseudo-distributions (as a consequence of the discrete spectrum). On the other hand, if the original equation had included couplings with $X_{n\pm2}^{m\pm2}$ we would have arrived at 5-term vector recursions (e.g., for biaxial spins, or not invoking secular approximations). Nevertheless, recurrences involving more than three terms can be 'folded' into 3-term form by introducing appropriate block vectors and matrices (appendix D.3). Alternatively, if the elements breaking the 3-term structure are suitably small, they can be treated iteratively (avoiding to enlarge dimensions) in a way similar to the forcing terms below.

7.2. The forcing terms (iterative calculations)

Equations $\kappa \mathrm{i}\Omega X_\kappa \sim (\mathrm{i}\Delta_0 + \mathcal{W}_0)X_\kappa + (\mathrm{i}\Delta_1 + \mathcal{W}_1)X_{\kappa-1}$ of section 6 can be manipulated analogously, as they inherit the structure of the original master equation. The main novelty is the forcing term $(\mathrm{i}\Delta_1 + \mathcal{W}_1)X_{\kappa-1}$, which will be handled here.

Recall that bold letters in equations (27), (28) stand for all X_n^m elements, to which we will have to add indices for perturbative order and harmonic. Then to avoid too baroque expressions we introduce the simplified notation $Y \equiv X_0^{(0)}$ and $Z \equiv X_1^{(1)}$. The zeroth-order

equation (27) can then be written as (cf equation (18))

$$
\begin{aligned}
0 = {}& i\Delta_{nm}^0 Y_n^m + \tfrac{i}{2} B_+^0 \big(\ell_m^+ Y_n^{m+1} - \ell_n^- Y_{n-1}^m\big) + \tfrac{i}{2} B_-^0 \big(\ell_m^- Y_n^{m-1} - \ell_n^+ Y_{n+1}^m\big) \\
& + (\mathcal{W}_0)_{n,n-1}^{m,m-1} Y_{n-1}^{m-1} + (\mathcal{W}_0)_{n,n}^{m,m} Y_n^m + (\mathcal{W}_0)_{n,n+1}^{m,m+1} Y_{n+1}^{m+1},
\end{aligned}
\tag{33}
$$

where index 0 stands for the absence of the probing field. The first line corresponds to $i\Delta_0 X_0^{(0)}$ and the second to $\mathcal{W}_0 X_0^{(0)}$. Similarly, the first-order equation (28) reads

$$
\begin{aligned}
i\Omega Z_n^m = {}& i\Delta_{nm}^0 Z_n^m + \frac{i}{2} B_+^0 \big(\ell_m^+ Z_n^{m+1} - \ell_n^- Z_{n-1}^m\big) + \frac{i}{2} B_-^0 \big(\ell_m^- Z_n^{m-1} - \ell_n^+ Z_{n+1}^m\big) \\
& + \big[(\mathcal{W}_0)_{n,n-1}^{m,m-1} Z_{n-1}^{m-1} + (\mathcal{W}_0)_{n,n}^{m,m} Z_n^m + (\mathcal{W}_0)_{n,n+1}^{m,m+1} Z_{n+1}^{m+1} \big] + f_n^m(\boldsymbol{Y}).
\end{aligned}
\tag{34}
$$

Again the custom terms stand for $i\Delta_0 X_1^{(1)}$ and $\mathcal{W}_0 X_1^{(1)}$ while the sources f_n^m account for $(i\Delta_1 + \mathcal{W}_1) X_0^{(0)}$. This is determined by the previous-order result $\boldsymbol{Y} = X_0^{(0)}$ and the field derivatives of $i\Delta$ and $\mathcal{W}$. Using $\delta\boldsymbol{B} \sim b(u_x, u_y, u_z)$ and $\Delta_{nm} = -[D(n+m) + B_z](n-m)$ we obtain

$$
\begin{aligned}
f_n^m = {}& -i(n-m)u_z Y_n^m + \frac{i}{2} u_+ \big(\ell_m^+ Y_n^{m+1} - \ell_n^- Y_{n-1}^m\big) + \frac{i}{2} u_- \big(\ell_m^- Y_n^{m-1} - \ell_n^+ Y_{n+1}^m\big) \\
& + u_z \big[(\mathcal{W}_1)_{n,n-1}^{m,m-1} Y_{n-1}^{m-1} + (\mathcal{W}_1)_{n,n}^{m,m} Y_n^m + (\mathcal{W}_1)_{n,n+1}^{m,m+1} Y_{n+1}^{m+1} \big],
\end{aligned}
\tag{35}
$$

where $u_\pm = u_x \pm i u_y$ and $(\mathcal{W}_1)_{n,n'}^{m,m'} \equiv d\big(\mathcal{W}_{n,n'}^{m,m'}\big)/dB_z$, because $\mathcal{W}$ only depends on B_z (recall that our relaxation term is approximate in $B_\pm$; section 4).

Now, to convert the $(2S+1)^2 \times (2S+1)^2$ systems (33) and (34) into vector recurrences, we proceed just as in section 7.1 for the parts $\kappa i\Omega X_\kappa \sim (i\Delta_0 + \mathcal{W}_0) X_\kappa$, while we introduce appropriate forcing vectors $\boldsymbol{f}_n$. This gives

$$
\mathbb{Q}_n^- \boldsymbol{c}_{n-1} + \hat{\mathbb{Q}}_n \boldsymbol{c}_n + \mathbb{Q}_n^+ \boldsymbol{c}_{n+1} = -\boldsymbol{f}_n, \qquad \hat{\mathbb{Q}}_n \equiv \mathbb{Q}_n - \kappa i\Omega \mathbb{I}.
\tag{36}
$$

Now $(\boldsymbol{c}_n)_m = Y_n^m$ or Z_n^m and $(\boldsymbol{f}_n)_m = f_n^m$, while $(\mathbb{Q}_n)_{mm'} = Q_{n,n}^{m,m'}$ and $\big(\mathbb{Q}_n^\pm\big)_{mm'} = Q_{n,n\pm1}^{m,m'}$ as above. The modified central matrix $\hat{\mathbb{Q}}_n$ ($\mathbb{I}$ is the identity) incorporates the left-hand sides $\kappa i\Omega X_\kappa$. The source terms (absent for $\kappa = 0$) can also be written as $\boldsymbol{f}_n = d_b \mathbb{Q}_n^- \boldsymbol{c}_{n-1}^{(\kappa-1)} + d_b \mathbb{Q}_n \boldsymbol{c}_n^{(\kappa-1)} + d_b \mathbb{Q}_n^+ \boldsymbol{c}_{n+1}^{(\kappa-1)}$, with $\boldsymbol{c}_n^{(\kappa-1)}$ the previous-order result and the matrices differentiated with respect to the probing field: $(\cdot)_1 \equiv d(\cdot)/db$.

Equation (36) has the canonical form permitting to apply directly the continued-fraction algorithm of appendix G. In addition, apart from perturbatively, the form (36) also follows from the original master equation $\dot{\boldsymbol{c}}_n = \mathbb{Q}_n^- \boldsymbol{c}_{n-1} + \mathbb{Q}_n \boldsymbol{c}_n + \mathbb{Q}_n^+ \boldsymbol{c}_{n+1}$ through Laplace transformation (for t-independent $\mathbb{Q}_n$). Then one just identifies $\hat{\mathbb{Q}}_n \equiv \mathbb{Q}_n - s\mathbb{I}$ (i.e., $\kappa i\Omega \to s$, the Laplace variable) and $\boldsymbol{f}_n \equiv \boldsymbol{c}_n(t=0) \sim \varrho(0)$. This would allow tackling initial-value problems (not forgetting the cautionary remarks of appendix D.3).

7.3. Spin response and susceptibilities

Once the recursions are solved we have *all* density-matrix elements $(\boldsymbol{c}_n)_m = \langle X_n^m \rangle = \varrho_{mn}$ and *any* observable can be obtained from the trace formula $\langle A \rangle = \sum_{nm} \varrho_{nm} A_{mn}$. For instance $\langle S_i \rangle = \sum_{nm} \langle n|S_i|m\rangle (\boldsymbol{c}_n)_m$, which connects directly the spin response with the continued-fraction results. To get explicitly the response to $\delta B = b\cos(\Omega t)$ we insert the expansion $X_n^m(t) \simeq Y_n^m + \frac{b}{2}\big(Z_n^m e^{+i\Omega t} + \tilde{Z}_n^m e^{-i\Omega t}\big)$ into the above average (cf equations (25) and (27), $X_0^{(0)} \to Y$ and $X_1^{(1)} \to Z$):

$$
\langle S_i \rangle = \sum_{nm} \langle n|S_i|m\rangle Y_n^m + \frac{b}{2}\left\{ \left[\sum_{nm} \langle n|S_i|m\rangle Z_n^m \right] e^{+i\Omega t} + \left[\sum_{nm} \langle n|S_i|m\rangle \tilde{Z}_n^m \right] e^{-i\Omega t} \right\}.
$$

Comparison with $\langle S_i \rangle = \langle S_i \rangle_0 + \frac{b}{2}(\chi e^{+i\Omega t} + \chi^* e^{-i\Omega t})$ gives the static response $\langle S_i \rangle_0$ and the dynamical susceptibility $\chi(\Omega)$. In terms of its real part χ' and imaginary part χ'' the time-dependent response is $\langle S_i \rangle(t) - \langle S_i \rangle_0 = b(\chi' \cos \Omega t + \chi'' \sin \Omega t)$. Proceeding to higher orders, as sketched in section 6, $X_0^{(0)} \rightarrow X_1^{(1)} \rightarrow X_2^{(2)} \rightarrow X_3^{(3)} \rightarrow \cdots$, the non-linear susceptibilities (higher harmonics) would follow similarly: $\chi^{(\kappa)}(\Omega) = \sum_{nm} \langle n|S_i|m \rangle [X_\kappa^{(\kappa)}]_n^m$.

8. Application to isotropic spins

Now we proceed to apply the discussed methods to solve the density-matrix equations for various systems. We will start with Garanin's master equation (21) for isotropic spins, $\mathcal{H} = -B \cdot S$, with a simple linear coupling to the bath $F = \eta \cdot S$. The bath is assumed Ohmic, $J(\omega) = \lambda \omega$, with rate function $W(\Delta) = \lambda \Delta / (e^{\Delta/T} - 1)$ (section 5.1). There are several analytical results for the static and dynamical response of isotropic spins, which will be used as a benchmark for the continued-fraction approach.

8.1. Matrix coefficients of the recurrences

Comparing the relaxation term (20) with the generic form (17) we identify the relaxation coefficients $\mathcal{W}_{n,n'}^{m,m'}$ of the isotropic spin. Using them in equation (21) for coefficients $\mathbb{Q}_n$ and the Zeeman level differences $\Delta_{nm} = -(n-m)B_z$, we have

$$\mathbb{Q}_n^- \begin{cases} Q_{n,n-1}^{m,m-1} = w_0 \ell_{n-1} \ell_{m-1} \\ Q_{n,n-1}^{m,m} = -(i/2)B_+ \ell_{n-1} \\ Q_{n,n-1}^{m,m+1} \equiv 0 \end{cases} \qquad \mathbb{Q}_n^+ \begin{cases} Q_{n,n+1}^{m,m-1} \equiv 0 \\ Q_{n,n+1}^{m,m} = -(i/2)B_- \ell_n \\ Q_{n,n+1}^{m,m+1} = w_0 e^{-y} \ell_n \ell_m \end{cases} \qquad (37)$$

$$\mathbb{Q}_n \begin{cases} Q_{n,n}^{m,m-1} = (i/2)B_- \ell_{m-1} \\ Q_{n,n}^{m,m} = -i(n-m)B_z - (w_0/2)\left[\left(\ell_n^2 + \ell_m^2\right) + e^{-y}\left(\ell_{n-1}^2 + \ell_{m-1}^2\right)\right] \\ Q_{n,n}^{m,m+1} = (i/2)B_+ \ell_m. \end{cases} \qquad (38)$$

Recall that $y = B_z/T$, the decay rate is $w_0 = \lambda T y/(1 - e^{-y})$, while $\ell_m = \ell_m^+$ and $\ell_{m-1} = \ell_m^-$ with $\ell_m^\pm = [S(S+1) - m(m \pm 1)]^{1/2}$. From these coefficients one also gets the derivatives $d_b \mathbb{Q}_n$ for the treatment of probing fields, $B \rightarrow B + b(t)u$, completing the specification of the 3-term recurrences (32) and (36).

8.2. Thermal equilibrium response

Analytical results. The statics of isotropic spins $\mathcal{H} = -B_z S_z$ can be studied in full analytically, giving us the opportunity to test the continued-fraction solution of the master equation. The *magnetization* $m_z \equiv \langle S_z \rangle$ is given by the Brillouin function $\mathcal{B}_S$:

$$m_z = S\mathcal{B}_S(\xi), \qquad \mathcal{B}_S(\xi) \equiv \left(1 + \frac{1}{2S}\right) \text{cth}\left[\left(1 + \frac{1}{2S}\right)\xi\right] - \frac{1}{2S} \text{cth}\left(\frac{1}{2S}\xi\right), \qquad (39)$$

with the scaled field variable $\xi = SB_z/T$ $(= Sy)$. For $SB_z \gg T$, $\mathcal{B}_S \rightarrow 1$ and saturation $m_z \simeq S$ is reached. The *longitudinal susceptibility* $\chi_\parallel \equiv \partial \langle S_z \rangle / \partial B_z$ follows using $(\text{cth}\, x)' = 1 - \text{cth}^2 x$ and $\partial_{B_z} = \partial_y/T$:

$$\chi_\parallel = \frac{S(S+1)}{T} - \left\{\left(S + \frac{1}{2}\right)^2 \text{cth}^2\left[\left(1 + \frac{1}{2S}\right)\xi\right] - \frac{1}{4}\text{cth}^2\left(\frac{1}{2S}\xi\right)\right\} \Big/ T. \qquad (40)$$
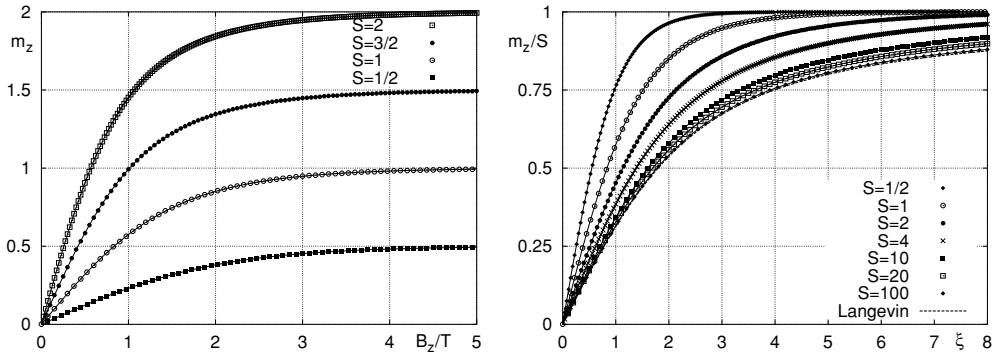
Figure 2. Magnetization $m_z = \langle S_z \rangle$ versus field of isotropic spins. Left panel: m_z versus B_z/T for various small S. Right panel: reduced magnetization m_z/S versus $\xi = SB_z/T$ for increasingly large S. The symbols are continued-fraction calculations and the lines Brillouin functions (39) (the dashed line is the classical limit $L(\xi) = \text{cth}(\xi) - 1/\xi$).
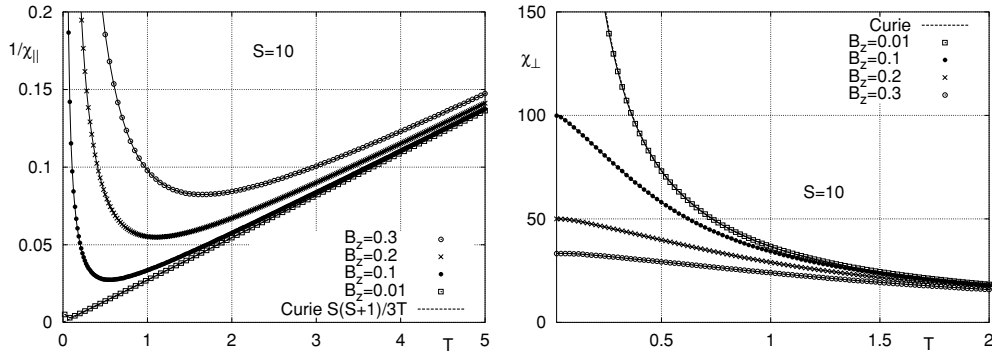
Figure 3. Temperature dependence of the susceptibilities of an isotropic $S = 10$ spin in various external fields. Left: reciprocal longitudinal response $1/\chi_\parallel$; the lines are Curie–Brillouin susceptibilities (40). Right: transverse response; lines $\chi_\perp = m_z/B_z$ (equation (41)). The symbols are continued-fraction results.

Expanding the hyperbolic cotangent as $\text{cth}\, x \simeq 1/x + x/3$, the second term goes over $-2S(S+1)/3T$ as $B_z \to 0$, completing the Curie law $\chi_0 = S(S+1)/3T$ for the initial (zero-bias) susceptibility of isotropic spins. On the other hand, the response to a probing field perpendicular to B_z is given by the *transverse susceptibility*:

$$\chi_\perp = m_z/B_z, \qquad m_z = \langle S_z \rangle. \tag{41}$$

Here we used Van Vleck's formula [55] to get $\chi_\perp \equiv \chi_{xx}$ with the transverse-field-dependent energy levels $\chi_{ii} = \mathcal{Z}^{-1} \sum_m \left[\beta(\partial_i \varepsilon_m)^2 - \partial_i^2 \varepsilon_m \right] e^{-\beta \varepsilon_m}$ where $\partial_i \varepsilon \equiv \partial \varepsilon/\partial B_i$. For $SB_z \ll T$, one has $m_z \simeq B_z \times S(S+1)/3T$, recovering Curie's law from this side.

Numerical results. Figure 2 shows the agreement of the continued-fraction results with analytical $\langle S_z \rangle$. The curves for small spins exhibit saturation to the corresponding S at large fields. Increasing S, up to $S = 100$, we can follow the evolution towards the *classical* Langevin magnetization $m_z/S \to \text{cth}(\xi) - 1/\xi$ (equation (39) with the leading terms $1 + 1/2S \simeq 1$ and $\text{cth}(\xi/2S) \simeq 2S/\xi$). At $S = 20$ the result is already close to the classical dependence. However, this depends on the field range observed; for quantum behaviour it is found whenever

the discreteness of the energy levels is important, and this can be attained by increasing sufficiently B_z.[5]

The agreement of the magnetizations, which is numerically exact, ensures agreement for the susceptibilities. Still we have computed $\chi_\parallel = \partial m_z / \partial B_z$ directly from the equilibrium fluctuations of the spin $\chi_\parallel = (\langle S_z^2 \rangle - \langle S_z \rangle^2)/T$, to check the proper continued-fraction obtainment of second-order moments $\langle S_i S_j \rangle = \sum_{nm} \langle n|S_i S_j|m\rangle (c_n)_m$. Figure 3 shows $1/\chi_\parallel$ versus temperature for a moderate spin. In a small B_z there is a straight-line dependence in almost all the range (Curie law $\chi_0^{-1} = 3T/S(S+1)$). Raising the field we observe deviations upwards (maximum in $\chi_\parallel$) at sufficiently low T. This occurs because $\chi_\parallel$ is the slope of the magnetization curve and, at high B_z/T, saturation $m_z \to S$ takes place and the slope drops to zero.

Figure 3 also displays the transverse susceptibility. For a quantum spin $\chi_\perp$ is not easily expressed in terms of averages in the absence of perturbation, so we resorted to applying directly a small transverse field and computing $\chi \sim \langle S_x \rangle / B_x$. The agreement with equation (41) is remarkable (recall that the relaxation term is approximate in the transverse field, section 4). We see how $\chi_\perp$ is reduced as T increases, approaching the Curie regime. At low T the magnetization saturates, $m_z \sim S$, and the curves tend to the constant values $\chi_\perp(T = 0) = S/B_z$.

8.3. Dynamical response

Let us turn now to the dynamics of isotropic spins. We will consider the response to probing fields $b\cos(\Omega t)$ parallel and perpendicular to the bias field B_z.

8.3.1. Analytical results. For $\delta \boldsymbol{B} \parallel \boldsymbol{B}$, on replacing $B_z \to B_z + b\cos(\Omega t)$ in the balance equations (19) (with the coefficients of section 5.1) and expanding to the first order in b one obtains equations determining the *longitudinal* susceptibility. They form a system of few coupled equations for small spins and can be solved analytically [31, 47, 56]. For $S = 1/2$ one finds the *Debye* form $[(\cdot)' \equiv \mathrm{d}(\cdot)/\mathrm{d}y;\ y = B_z/T]$

$$\chi_\parallel(\Omega) = \frac{m_z'}{T} \frac{\Gamma}{\Gamma + i\Omega}, \qquad \Gamma = w_0(1 + e^{-y}), \tag{42}$$

where $m_z = \frac{1}{2}\,\mathrm{th}\left(\frac{1}{2}y\right)$ and m_z'/T is the equilibrium response. The characteristic *relaxation time* is $\tau = 1/\Gamma$. As the decay rate is $w_0 = W(-y)$, with $W(y) = \lambda T y/(e^y - 1)$, one has $\Gamma = W(-y) + W(y)$ (see appendix E). Next, for $S = 1$ the susceptibility can be written as [31]

$$\chi_\parallel(\Omega) = \frac{m_z'}{T} \frac{\Lambda_1 \Lambda_2 + i\Omega\Gamma_1}{(\Lambda_1 + i\Omega)(\Lambda_2 + i\Omega)}. \tag{43}$$

Here $\Gamma_1 = \Gamma(2\,\mathrm{ch}\,y + 1)/(\mathrm{ch}\,y + 2)$, with $\Gamma = W(-y) + W(y)$ again, and $\Lambda_{1,2}$ are the non-zero eigenvalues of the matrix associated with the system of balance equations $\Lambda_{1,2} = \Gamma\left[2\,\mathrm{ch}\left(\frac{1}{2}y\right) \mp 1\right]/\mathrm{ch}\left(\frac{1}{2}y\right)$ ($\Lambda_0 = 0$ corresponds to the thermal equilibrium solution). This formula can be expressed as the sum of two Debye terms (cf equation (48) below). But as Λ_1 is numerically close to Γ_1, the susceptibility is nearly single Debye $\simeq m_z'/T\ \Gamma_1/\Gamma_1 + i\Omega$ with an effective relaxation time $\tau \sim 1/\Gamma_1$.

---

[5] For the statics, we use a weak spin–bath coupling $\lambda = 10^{-9}$ in the density-matrix equation (21). We know that in the absence of the transverse field its diagonals are decoupled (after the rotating-wave approximation). Then detailed balance $W(\Delta) = e^{-\Delta/T} W(-\Delta)$ ensures that the Gibbs distribution is its statiorary solution. Thus the static continued-fraction results must be independent of λ.

For arbitrary S the longitudinal relaxation comprises $2S + 1$ modes [56] (the rank of the matrix associated with the balance equations). In general, their amplitudes a_i and rates $0 = \Lambda_0 \leqslant \Lambda_1 \leqslant \cdots \leqslant \Lambda_{2S}$ need to be obtained numerically [47]. This makes it difficult to derive closed expressions for the susceptibility, $\chi(\Omega) = \chi \sum_{i=1}^{2S} a_i / (1 + \mathrm{i}\Omega/\Lambda_i)$, but still something can be said on the relaxation time. An overall measure is provided by the *integral relaxation time*, $\tau_{\mathrm{int}} \equiv \int_0^\infty \mathrm{d}t\, \delta M(t)/\delta M(0)$, where $\delta M(t)$ is the response to a small field change δB_z at $t = 0$ [4]. Its advantage is that one can bypass the computation of the time constants and amplitudes [44, 45, 47] by getting τ_{int} directly from the low-frequency susceptibility $\chi(\Omega) \simeq \chi(1 - \mathrm{i}\Omega\tau_{\mathrm{int}} + \cdots)$ which can be obtained in a closed form (see appendix F for explicit expressions for τ_{int}).

Finally, to have some analytical formula for the susceptibility at arbitrary S, one introduces a *single-relaxation time* approximation

$$\chi_\parallel(\Omega) = \frac{m_z'}{T} \frac{1}{1 + \mathrm{i}\Omega\tau_{\mathrm{int}}}. \tag{44}$$

This is possibly the most popular expression in the modelling of relaxation experiments. By construction this heuristic form is correct at low frequencies. The accuracy for arbitrary Ω will have to be assessed in each problem addressed.

8.3.2. Longitudinal response. Figure 4 displays susceptibility spectra for a spin $S = 1/2$ in a number of fields, showing the agreement between the analytical and continued-fraction results (again numerically exact). The curves go down as the field is increased. This is mainly due to the reduction of the equilibrium part of the response m_z'/T (equation (42)), which is the slope of the magnetization and decreases with increasing B_z. The peaks of the imaginary part χ'', and the maximum slope of the real part χ', occur at $\Omega \sim \Gamma$. Then, as the relaxation rate $\Gamma = W(-y) + W(y)$ increases with B_z (appendix E), the curves shift to higher frequencies. Finally, as the response comprises a single Debye factor $\chi \sim 1/(1 + \mathrm{i}x)$, plotting imaginary versus real parts (Cole–Cole or Argand representation) gives perfect semicircles [57].

The longitudinal response for $S = 1$ is also shown in figure 4. In comparison with spin-1/2, the susceptibilities are higher and more sensitive to the bias field. This can be related with the magnetization curves of figure 2, which for $S = 1$ have larger slopes and change faster with B_z (the parameter coupling to the field, i.e., S, is larger now). On the other hand, as the deviation of equation (43) from a single Debye is small, the Cole–Cole plots are nearly semicircular.

For arbitrary S, finally, we compare the continued-fraction results with the heuristic formula $\chi_\parallel(\Omega) = \chi_\parallel/(1 + \mathrm{i}\Omega\tau_{\mathrm{int}})$. Figure 5 shows that the agreement is very good in general, implying that the relaxation modes Λ_i are quite grouped (on a logarithmic scale). There are only small deviations at the peaks in intermediate fields ($\xi \sim 2$–4), in accordance with Garanin's findings in [31]. On the other hand, this figure (and figure 2) illustrates that in order to reach the classical asymptotes, the quantities need to be scaled appropriately[6].

8.3.3. Paramagnetic resonance. We conclude with the response to transverse probing fields. These incorporate $S_\pm$ in the Hamiltonian, not commuting with the dominant S_z-dependent part,

---

[6] We used the scalings $B_z \to SB_z/T$, $m_z \to m_z/S$ and $\chi \to \chi/S(S+1)$. In general, we increase S keeping the amount of Zeeman energy and the anisotropy barriers constant (and hence finite at $S \to \infty$). For the Hamiltonian $\mathcal{H} = -DS_z^2 - \boldsymbol{B} \cdot \boldsymbol{S}$ this amounts to fixing DS^2 and SB, while introducing more levels with S (their spacing decreases as $\Delta \sim 1/S$, appendix A). Correspondingly [58, 47, appendix A], frequency and damping are scaled as $\Omega \propto 1/S$ and $\lambda \propto 1/S$ (recall that $\lambda \sim \lambda_{\mathrm{LL}}/2S$). Alternatively one can use the scaling combination Ω/λ (or some $\Omega\tau$), as we did here.
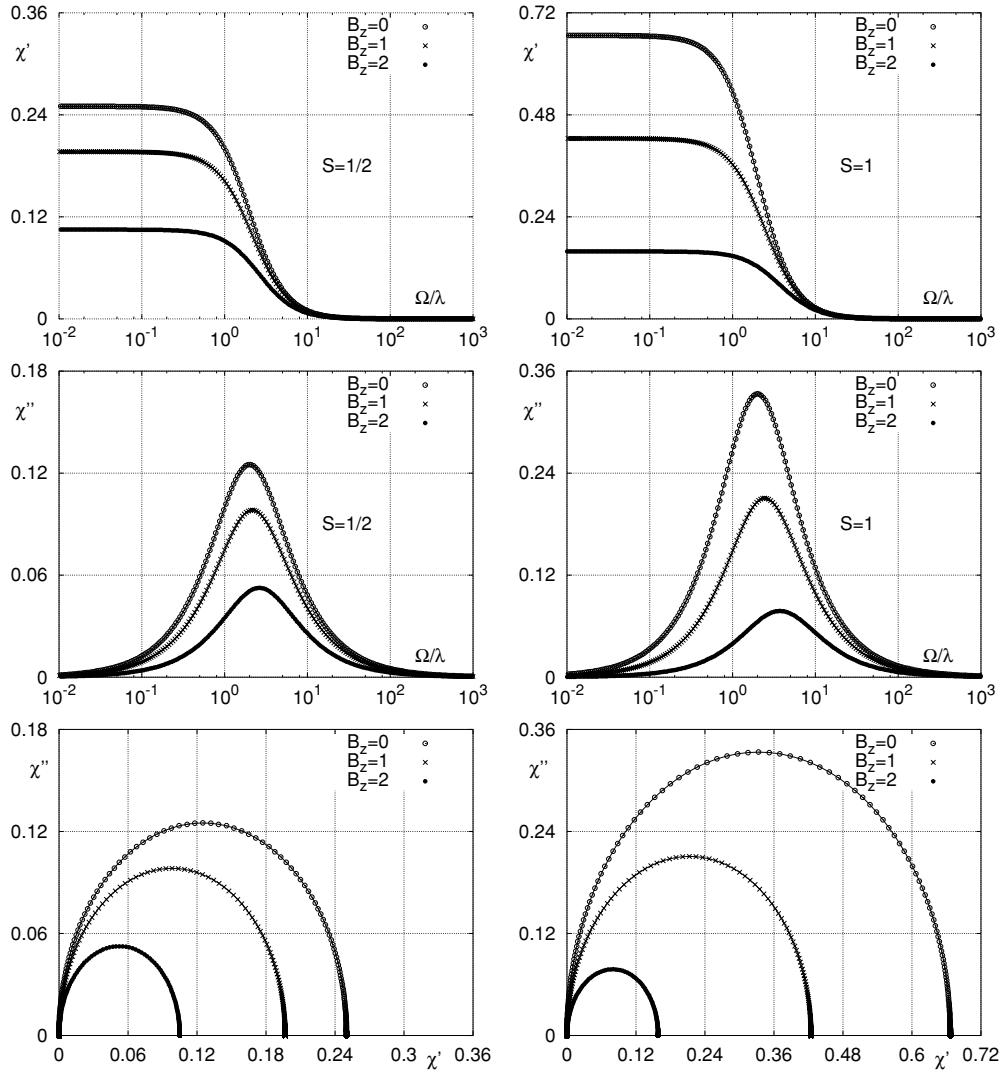
Figure 4. Dynamical susceptibility $\chi_{\parallel}(\Omega)$ for $S = 1/2$ (left panels) and $S = 1$ (right panels). The temperature is $T = 1$, $\lambda = 10^{-9}$, and results in various fields are shown. The lines are the analytical expressions (42) and (43) and the symbols are continued-fraction results. The different panels are the real part χ' (top), imaginary part χ'' (middle) and Cole–Cole plot χ'' versus χ' (bottom panels).

and provoking transitions $|m\rangle \rightarrow |m \pm 1\rangle$ between the unperturbed levels. These transitions result in peaks at the frequencies $\Delta_{m,m\pm1} = \varepsilon_m - \varepsilon_{m\pm1}$ in the imaginary part of the susceptibility [48] (absorption line shape). Classically the phenomenon corresponds to the matching of the oscillating field with the Larmor precession of the spin. Finally, as the quantum transverse response $\langle S_{\pm} \rangle = \sum_m \ell_m^{\pm} \langle X_{m\pm1}^m \rangle$ involves off-diagonal elements of ϱ (coherences), one refers to the precession in transverse fields as *coherent* dynamics.

As the level spacings of an isotropic spin are all equal $\Delta_{m,m\pm1} = \pm B_z$, the phenomenology for the different S is qualitatively similar. Figure 6 shows the susceptibility $\chi_{\perp} \equiv \chi_{xx}$ for
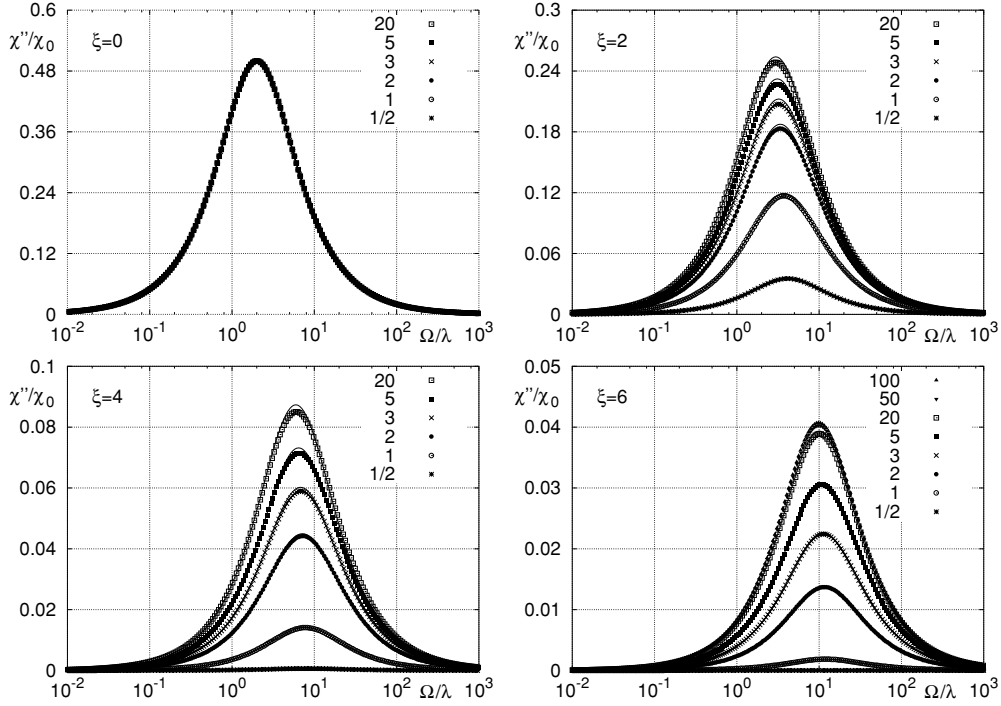
Figure 5. Imaginary part of the susceptibility for $S = 1/2, 1, 2, 3, 5, 20$. Again $T = 1$ whereas the fields are chosen to fix $\xi = SB_z/T = 0, 2, 4, 6$ for the different S. The solid lines are the single-relaxation time approximation (44) and the symbols are continued-fraction calculations (normalized by the Curie $\chi_0 = S(S + 1)/3T$). For $\xi = 6$ we also display numerical results for $S = 50$ and 100 (rhombi), indicating convergence to a classical limit.

$S = 1/2$, for which we have exact formulae [56]

$$\chi_\perp(\Omega) = \frac{m_z}{2} \left(\frac{1}{B_z - \Omega + \mathrm{i}\Gamma_2} + \frac{1}{B_z + \Omega - \mathrm{i}\Gamma_2} \right), \qquad \Gamma_2 = \frac{1}{2} w_0 (1 + \mathrm{e}^{-y}). \tag{45}$$

(To get this equation one has to solve the full density-matrix equation (21); for $S = 1/2$ the form coincides with that obtained from phenomenological Bloch equations identifying $T_2 = 1/\Gamma_2$.) The continued-fraction results and equation (45) agree to all computed figures. In particular, the numerical results duly fulfil the basic relation $\chi(-\Omega) = [\chi(\Omega)]^*$, yielding even $\chi'(\Omega)$ and odd $\chi''(\Omega)$. The imaginary part shows peaks at $|\Omega| = B_z$, the level separation, accompanied by zigzag with sign change of the real part. Decreasing the spin–bath coupling λ the absorption peaks become narrower and higher, as in a forced and damped oscillator. Here, this can also be attained by changing T (right panel). These behaviours, captured by the line width Γ_2 in equation (45), reflect the 'smearing out' of the energy levels due to the bath coupling.

With this simple example we have introduced the basic phenomenology of magnetic resonance and some factors influencing it. On the other hand, the perfect agreement of the continued-fraction results with the exact solution lends confidence to our handling of the non-diagonal elements of ϱ, required to compute $\langle S_\pm \rangle = \sum_m \ell_m^\pm \varrho_{m,m\pm1}$. This is important for the subsequent application to spins in the anisotropy potential, where there are less analytical expressions to compare with.
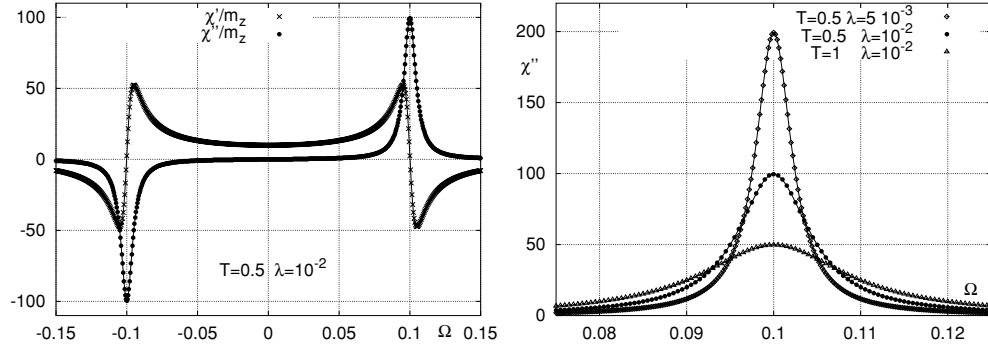
Figure 6. Transverse susceptibility $\chi_\perp(\Omega)$ of an isotropic spin $S = 1/2$ in a magnetic field $B_z = 0.1$. The lines are equation (45) and the symbols are continued-fraction results. Left: real and imaginary parts for $\lambda = 0.01$ at $T = 0.5$. Right: detail of the effects of the damping (halved to $\lambda = 0.005$) and of the temperature (doubled to $T = 1$) on the absorption line shape $\chi_\perp''(\Omega)$.

9. Application to anisotropic spins (superparamagnets)

Now we consider spins with a Hamiltonian $\mathcal{H} = -DS_z^2 - \boldsymbol{B} \cdot \boldsymbol{S}$ and a quadratic coupling $F \sim S_z S_\pm$, motivated by the spin–lattice interaction in (super)paramagnets [32, 36]. Correspondingly, we use the rate function $W(\Delta) = \lambda \Delta^3/(e^{\Delta/T} - 1)$ of a $\alpha = 3$ super-Ohmic phonon bath. At variance with the uniform Zeeman spectrum, the anisotropy results in non-equispaced levels (figure 1) and hence in several rates $W_{m|m\pm1} = W(\Delta_{m,m\pm1})$. Thus this problem is a spin analogue of translational quantum Brownian motion in non-harmonic potentials.

9.1. Elements of the density-matrix recurrences

To solve the density-matrix equation (22) by continued fractions we convert it, as explained in section 7.2, into a vector 3-term recurrence of the form $\mathbb{Q}_n^- \boldsymbol{c}_{n-1} + \mathbb{Q}_n \boldsymbol{c}_n + \mathbb{Q}_n^+ \boldsymbol{c}_{n+1} = -\boldsymbol{f}_n$, with $(\boldsymbol{c}_n)_m = \varrho_{mn}$. The matrix coefficients $\mathbb{Q}_n$ comprise Hamiltonian and relaxational contributions. For this problem they are obtained comparing equations (22) and (30) (we include $\Delta_{nm} = -[D(n+m) + B_z](n-m)$):

$$
\mathbb{Q}_n^- \begin{cases}
Q_{n,n-1}^{m,m-1} = \frac{1}{2}\bar{\ell}_{n-1}\bar{\ell}_{m-1}(W_{n|n-1} + W_{m|m-1}) \\
Q_{n,n-1}^{m,m} = -(\mathrm{i}/2)B_+\ell_{n-1} \\
Q_{n,n-1}^{m,m+1} \equiv 0
\end{cases}
$$

$$
\mathbb{Q}_n \begin{cases}
Q_{n,n}^{m,m-1} = (\mathrm{i}/2)B_-\ell_{m-1} \\
Q_{n,n}^{m,m} = -\mathrm{i}[D(n+m) + B_z](n-m) \\
\qquad\quad - \frac{1}{2}\left(\bar{\ell}_n^2 W_{n+1|n} + \bar{\ell}_m^2 W_{m+1|m}\right) - \frac{1}{2}\left(\bar{\ell}_{n-1}^2 W_{n-1|n} + \bar{\ell}_{m-1}^2 W_{m-1|m}\right) \\
Q_{n,n}^{m,m+1} = (\mathrm{i}/2)B_+\ell_m
\end{cases}
$$

$$
\mathbb{Q}_n^+ \begin{cases}
Q_{n,n+1}^{m,m-1} \equiv 0 \\
Q_{n,n+1}^{m,m} = -(\mathrm{i}/2)B_-\ell_n \\
Q_{n,n+1}^{m,m+1} = \frac{1}{2}\bar{\ell}_n\bar{\ell}_m(W_{n|n+1} + W_{m|m+1}).
\end{cases}
$$

Recall that the replacement $\ell_m \rightarrow \bar{\ell}_m = (2m+1)\ell_m$ in the relaxation parts comes from S_z in $F \sim \{S_z, S_\pm\}$, leading to 'position-dependent' damping. The field derivatives of these
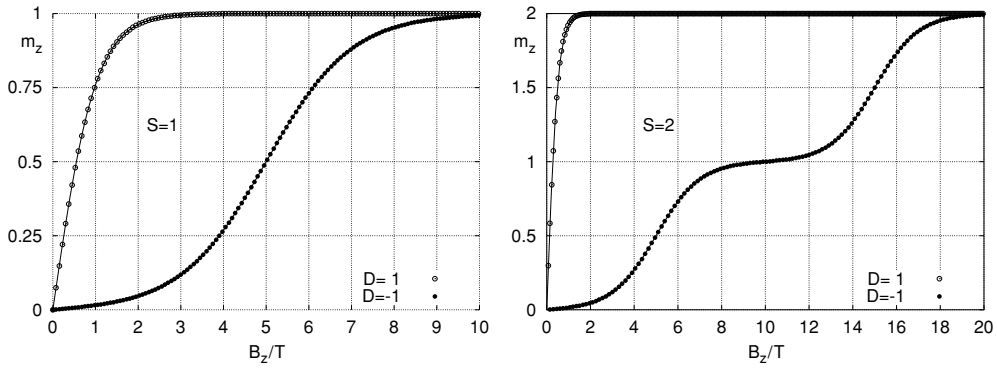
Figure 7. Magnetization curves of anisotropic spins with $S = 1$ (left) and $S = 2$ (right) both for positive and negative D at $T = 0.2$. Lines: Gibbsian formulae (46); symbols: continued-fraction results (with $\lambda = 10^{-9}$; see footnote 5 in section 8.2).
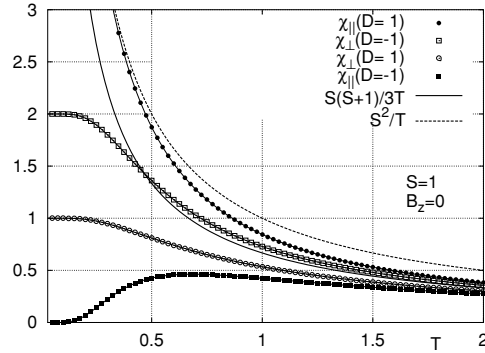
Figure 8. Equilibrium susceptibilities versus temperature of $S = 1$ spins with $D = 1$ (circles) and $D = -1$ (squares). We show longitudinal responses (full symbols) and transverse ones (open), together with equations (47) (thin lines). The thick solid line is Curie law, approached by all curves at high temperatures, and the dashed line is the Ising asymptote (for $\chi_{\parallel}(D > 0)$).

coefficients give the source terms $\boldsymbol{f}_n$ for the treatment of probing fields (see appendix E for dW/dB_z); then $\mathbb{Q}_n \rightarrow \mathbb{Q}_n - \kappa i \Omega \mathbb{I}$. With the density-matrix recurrence (36) so specified we can now apply the continued-fraction algorithm of appendix G to solve it.

9.2. Thermal equilibrium response

Again we begin discussing briefly the static properties in a longitudinal field. Compact expressions for the magnetization $m_z = \mathcal{Z}^{-1} \sum_m m \, e^{-\beta \varepsilon_m}$ follow for small spins. Introducing $d = D/T$ and $y = B_z/T$, we have $-\beta \varepsilon_m = dm^2 + ym$. Then for spin-1/2 $m_z = \frac{1}{2}(e^{y/2} - e^{-y/2})/(e^{y/2} + e^{-y/2})$, equal to the isotropic result (as D enters in the two levels equivalently). However, for $S = 1$ and 2 the magnetizations read

$$\langle S_z \rangle = \frac{2e^d \, \text{sh} \, y}{1 + 2e^d \, \text{ch} \, y} \qquad \langle S_z \rangle = \frac{2e^d \, \text{sh} \, y + 4e^{4d} \, \text{sh} \, (2y)}{1 + 2e^d \, \text{ch} \, y + 2e^{4d} \, \text{ch} \, (2y)}, \qquad (46)$$

which are valid for both $D > 0$ (easy-axes anisotropy) and $D < 0$ (easy plane; then the energy levels of figure 1 are turned upside down). Note that the $m = 0$ level does not contribute to $\sum_m m \, e^{-\beta \varepsilon_m}$ but contributes 'phase space' in the partition function $\mathcal{Z} = \sum_m e^{-\beta \varepsilon_m}$.

For $D > 0$ the states with $m = \pm S$ have the lowest energies in weak fields and are only separated by $2B_z S$. Then the magnetization curves have the convex features of the isotropic-spin case (figure 7, open symbols). In contrast, for $D < 0$ the curves depart from zero slowly (exponentially); the low-field ground state is then $m = 0$, well separated from the first excited level (by $|D| - B_z$). Indeed, for $S = 2$ and $D < 0$, when the field makes $m = 1$ the new ground state, the magnetization is again stabilized at $m_z \simeq 1$ until it 'jumps' to $m_z \simeq 2$. The jumps become steeper as T is decreased.

The longitudinal susceptibility for $S = 1$ follows by differentiating m_z in equation (46); the transverse response $\chi_\perp$ can be obtained from Van Vleck's formula (section 8.2). The results for the initial (zero-bias) susceptibilities are

$$\chi_\parallel = \frac{1}{T} \frac{2}{2 + \mathrm{e}^{-D/T}}, \qquad \chi_\perp = \frac{2}{D} \frac{1 - \mathrm{e}^{-D/T}}{2 + \mathrm{e}^{-D/T}}, \qquad (S = 1). \tag{47}$$

At high T both expressions recover the isotropic susceptibility: $\chi_\parallel|_{d=0} = \chi_\perp|_{d=0} = 2/3T$ (here $S(S + 1) = 2$). At low temperature one has $\chi_\parallel|_{d\to\infty} = 1/T$ for $D > 0$ (2-state like) in accordance with $m_z \to$ th $y \sim m_z|_{S=1/2}$. Thus in both limit ranges $\chi_\parallel$ obeys $1/T$ laws, with the factor $1/\left(1 + \frac{1}{2}\mathrm{e}^{-D/T}\right)$ governing the intermediate T crossover between the isotropic-spin and Ising regimes. In contrast, for $D < 0$, the longitudinal susceptibility goes to zero exponentially at low T. Again this is due to the $m = 0$ ground state for easy-plane anisotropy. Finally, as for the transverse response at low T, it tends to the constant limits $\chi_\perp|_{d\to\infty} = 1/D$ and $\chi_\perp|_{d\to-\infty} = 2/|D|$.

Textbook examples of the longitudinal and transverse susceptibilities [55] are displayed in figure 8, showing the agreement between the analytical expressions and the continued-fraction results (the longitudinal obtained as $\chi_\parallel = \left(\langle S_z^2\rangle - \langle S_z\rangle^2\right)/T$ and the transverse from $\chi_\perp(\Omega)$ using a small $\Omega/\lambda = 10^{-3}$; cf section 8.2). This agreement, together with the magnetization curves of figure 7, indicates that we are properly handling a quantum system with non-equispaced levels, as well as its transverse response, which requires off-diagonal density-matrix elements.

9.3. Dynamical response

9.3.1. Analytical results. Again exact expressions can be obtained for small S from the balance equations (19), with coefficients $\mathcal{W}_m^- = W_{m|m-1}\bar{\ell}_{m-1}^2$, $\mathcal{W}_m = -\left(\bar{\ell}_m^2 W_{m+1|m} + \bar{\ell}_{m-1}^2 W_{m-1|m}\right)$ and $\mathcal{W}_m^+ = W_{m|m+1}\bar{\ell}_m^2$. For $S = 1/2$ the coupling model considered does not produce relaxation (see appendix B). The first non-trivial case is $S = 1$, whose longitudinal susceptibility comprises two Debye factors [47]

$$\chi_\parallel(\Omega) = \frac{m_z'}{T}\left(\frac{a}{1 + \mathrm{i}\Omega/\Lambda_1} + \frac{1 - a}{1 + \mathrm{i}\Omega/\Lambda_2}\right), \qquad a = \frac{\Lambda_2 - \Lambda_{\mathrm{eff}}}{\Lambda_2 - \Lambda_1}. \tag{48}$$

Here Λ_i are eigenvalues of the balance-equations matrix,

$$\Lambda_0 = 0, \qquad \Lambda_{1,2} = (\Gamma_+ + \Gamma_-) \mp \sqrt{(\Gamma_+ - \Gamma_-)^2 + 4w_+ w_-}, \tag{49}$$

with the rates $\Gamma_\pm = 2[W(\Delta_{\pm 1,0}) + W(-\Delta_{\pm 1,0})]$ and transition probabilities $w_\pm = P_{\pm 1|0} = 2W(\Delta_{\pm 1,0})$ (recall that $W(\Delta) = \lambda\Delta^\alpha/(\mathrm{e}^{\Delta/T} - 1)$, $\Delta_{\pm 1,0} = -(D \pm B_z)$, and $\bar{\ell}_{\pm 1,0} = \pm\sqrt{2}$). The amplitude $a \in [0, 1]$ controlling the weights of the two summands involves $\Lambda_{1,2}$ and $\Lambda_{\mathrm{eff}} = (w_+ + w_-)/\mathcal{Z}m_z'$, the initial decay rate of the magnetization [47]. As $\mathcal{Z}m_z' = 2(\mathrm{ch}\, y + 2\mathrm{e}^d)/(2\,\mathrm{ch}\, y + \mathrm{e}^{-d})$ we have $\Lambda_{\mathrm{eff}} \to \Gamma_1$ as $D/T \to 0$, recovering the susceptibility of isotropic $S = 1$ spins (equation (43)). We are not aware of exact results for $\chi_\parallel(\Omega)$ of larger spins or for the transverse dynamical response with $D \neq 0$.
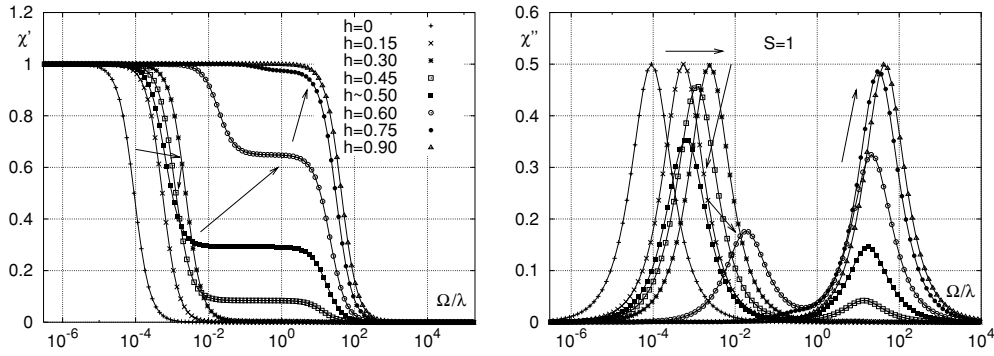
Figure 9. Longitudinal susceptibility spectra of an anisotropic $S = 1$ spin with $D = 1$ and $\lambda = 10^{-9}$ at $T = 0.1$ and various $h = B_z/2DS$, below and above barrier disappearance $B_c = D$ ($\sigma = 10, \xi = h \cdot 2\sigma = 0 \rightarrow 18$). Lines: exact two-mode equation (48); symbols: continued-fraction results; the arrows trace the field evolution. The susceptibility is normalized by the equilibrium $\Omega \rightarrow 0$ value.
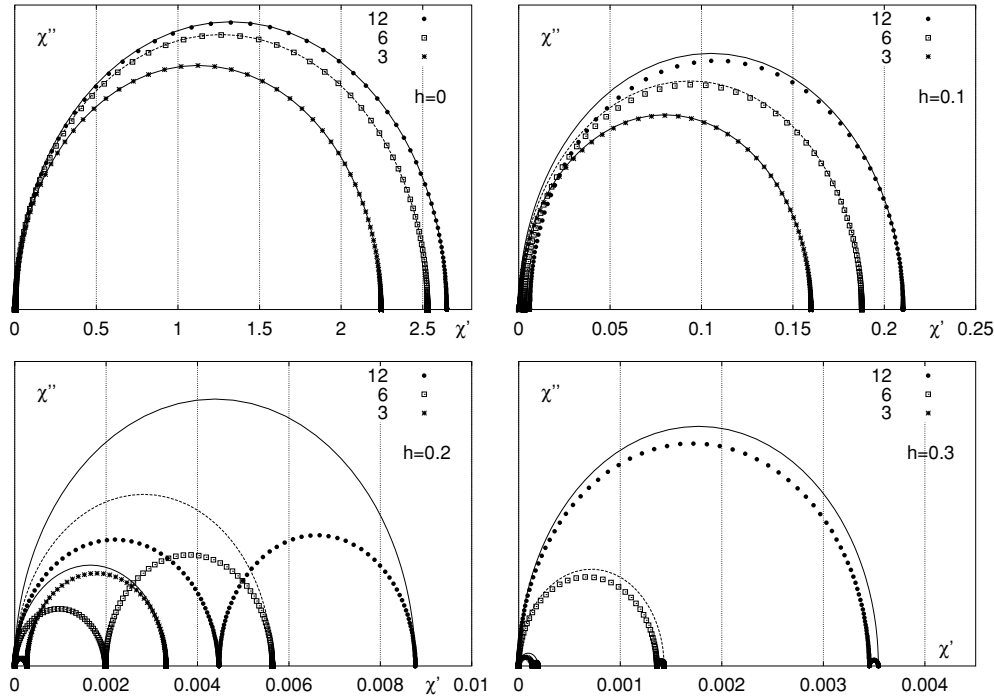
Figure 10. Cole–Cole plot of the longitudinal susceptibility of spins $S = 3, 6, 12$. The anisotropy parameter D is adjusted to fix $\sigma = DS^2/T = 10$ and the fields such that $\xi = SB_z/T = 0, 2, 4, 6$ ($h = 0, 0.1, 0.2, 0.3$). The lines are single Debye approximations and the symbols are continued-fraction results. The susceptibilities are scaled by $\chi_0 = S(S+1)/3T$ and the y-axis range is half the x-axis one.

9.3.2. Longitudinal response. As the range of parameters that can be explored is wide, we concentrate on low temperatures (and eventually, weak fields), the experimentally most interesting range in superparamagnets. It is convenient to introduce *reduced* anisotropy and field parameters

$$\sigma = |D|S^2/T, \qquad \xi = SB_z/T, \qquad h = \xi/2\sigma. \qquad (50)$$

The latter is B_z in units of $2|D|S$ which is of the order of the anisotropy field at the minima or the field for barrier disappearance (appendix A). As mentioned before, when comparing different S we scale parameters keeping σ and ξ fixed.

Let us begin with $S = 1$. Its dynamical susceptibility is displayed in figure 9 showing the full agreement between the analytical and numerical results. The curves evidence two relaxation modes $((2S + 1) - 1$, the equilibrium $\Lambda_0 = 0)$. Inspecting the structure of the corresponding eigenvectors [47], the low-frequency mode, Λ_1, can be associated with overbarrier crossings and the faster mode, Λ_2, with transitions between neighbouring levels $(\pm 1 \leftrightarrow 0$, intra-well dynamics). The overbarrier process dominates the response at weak fields; the intra-well is active but by symmetry its contribution to $\langle S_z \rangle$ practically cancels out (but not to $\langle S_z^2 \rangle$, the Kerr relaxation observable). Increasing B_z the spectrum loses the potential barrier at $B_c = D$ $(h_c = 1/2)$ and the fast transitions between adjacent states take over. For $B_z \gtrsim D$ the two modes are still separated, because the levels are not equispaced yet. Finally at high enough fields a Zeeman spectrum is approached and the isotropic susceptibility recovered (equation (43)); then the two modes are close (in frequency) and $\chi(\Omega)$ approaches again a single Debye form.

Let us now address the response of larger spins. Figure 10 shows that, although we should be finding $2S$ modes in $\chi(\Omega)$, they appear gathered in two main groups: the overbarrier mode Λ_1 and a bunch of high-frequency modes, related to intra-well transitions. This, in turn, leads to a phenomenology akin to that of $S = 1$. In this figure, we have chosen the Argand plot $(\chi''$ versus $\chi')$ where competing modes are resolved in two neat semicircles. They evolve into one in the limits of low and high field. In the low B_z regime the response is dominated by the overbarrier dynamics and there is a good agreement with a single Debye form $\chi(\Omega) = \chi/(1 + i\Omega\tau)$, with $\tau \sim 1/\Lambda_1$. But in contrast to $S = 1$, the intra-well modes are clearly manifested at fields h^* well below the field of barrier disappearance $h_c = 1 - 1/2S$ (equation (A.5)). Indeed, in the classical limit it was estimated that above only $h^* \sim 0.17$ the fast modes can significantly compete with the overbarrier process [59] due to the thermal depopulation of the upper well (cf figure 1). For large S (say $S \gtrsim 10$) we obtain h^* approaching such classical result. In addition, we see that the onset of the intra-well modes depends on the spin value. That is, $h^* = h^*(S)$, increasing for decreasing S. This seems natural because the results should recover $h^* \sim 0.5$ as $S \to 1$. Equivalently, at a fixed h the semicircle of the fast modes (the left one) is less developed the smaller the S is (panel $h = 0.2$). Eventually, at large B_z a single Debye again describes $\chi(\Omega)$ for all S. (For further discussion on $h^*(S)$, the modes interplay and analytical approximations, see [47].)

9.3.3. Superparamagnetic blocking. Finally we present the results at low fields, the range most studied in nanomagnets ($2DS \sim 10$ T in Mn_{12}) in a way closer to experiment [60, 61]. There one varies T at a fixed Ω, because the exponential dependence of the relaxation time $\tau \propto \exp(\Delta U/T)$ permits one to span various decades in $\Omega\tau$ in an easier way. The results show the phenomenology of superparamagnetic blocking—a maximum in the magnitude of the response at some intermediate Ω-dependent temperature (figure 11). This is different in nature from the maxima exhibited by the *equilibrium* $\chi_\parallel$ for $D < 0$, or for $D > 0$ in an external field (figures 3 and 8). The dynamical blocking is due to the competition of τ with $1/\Omega$ and the two-fold rolex played by T. It unblocks the overbarrier transitions at low temperatures, enabling the spins to follow the oscillating field $b\cos(\Omega t)$, but sufficiently high T also provokes the thermal misalignment of the spins from the field direction, degrading the response.
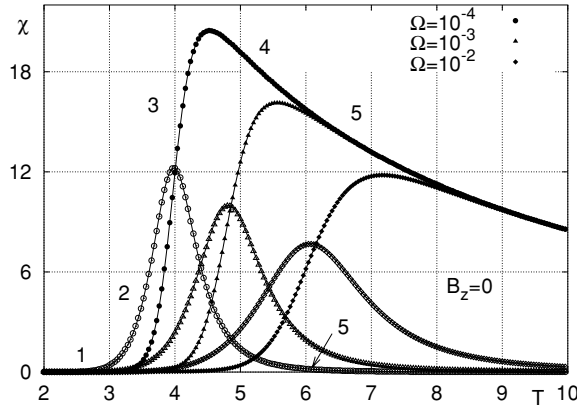
Figure 11. Dynamical susceptibility $\chi_\parallel$ versus temperature of an anisotropic $S = 10$ spin with $D = 0.5$ at several frequencies (in units of λ/D^2). Real parts (solid symbols), imaginary parts (open); single Debye equation (44) (lines). The numbers by the $\Omega = 10^{-4}$ curves correspond to the regimes discussed in the text. Considering D and T given in Kelvin, the values used are close to those of Mn_{12}.

Let us follow the process in some detail. (1) At low temperatures, $\tau \gg 1/\Omega$, the probability of overbarrier crossings is negligible and the dynamics consists of transitions at the bottom of the wells (with a small averaged projection onto the field). (2) Increasing T the spins appreciably depart from the minima, and the response starts to rise with T. However, as the thermoactivation is not efficient enough, the response $\langle S_z \rangle(t) \sim b(\chi' \cos \Omega t + \chi'' \sin \Omega t)$ sizably lags behind the field, as manifested by the large χ''. (3) At higher temperatures the overbarrier mechanism becomes more efficient; the response continues increasing, but becoming more in-phase with the excitation (χ' dominates). (4) If T is further increased, however, the thermal agitation also provokes misalignment of the spins from the field direction. Then the magnitude of the response exhibits a maximum and starts to decrease; this occurs at a temperature T_b such that $\tau(T_b) \sim 1/\Omega$. (5) Eventually, at high T, the spins quickly adjust to the equilibrium distribution corresponding to the instantaneous field. Then χ' goes over the equilibrium susceptibility ($\propto 1/T$) while χ'' drops to zero. Note finally that, in agreement with the previous subsection, all this low-field phenomenology is well described by a single Debye form, as figure 11 shows[7].

9.3.4. Paramagnetic resonance of anisotropic spins.

We conclude with the spin-resonance behaviour of quantum superparamagnets [58]. Recall that a field oscillating perpendicular to the anisotropy axis provokes transitions $|m\rangle \to |m \pm 1\rangle$ between the unperturbed levels. Computing the response along such a field $\langle S_\pm \rangle = \sum_m \ell_m^\pm \varrho_{m,m\pm 1}$ requires off-diagonal density-matrix elements and falls outside a Pauline master equation for the populations ϱ_{mm}.

The induced transitions result in peaks in the absorption line shape $\chi''(\Omega)$ at frequencies $\Delta_{m,m\pm1}$. For an isotropic spin all level differences were equal $\Delta_{m,m+1} = B_z$. Here, however, the anisotropy yields non-equispaced levels $\Delta_{m,m+1} = D(2m + 1) + B_z$ and one would expect multiple peaks in $\chi''(\Omega)$, with the corresponding zigzags in real part $\chi'(\Omega)$. At the zero field the

---

[7] For low Ω we have found numerical instabilities of the continued-fraction results with very large $\Delta U/T$. Some accuracy problems also arise in isotropic spins at very large B_z/T. They can be attributed to the exponential dependences of the relaxation rates, giving tiny numbers at certain critical places; this is known to happen in the classical case under the same limit conditions.
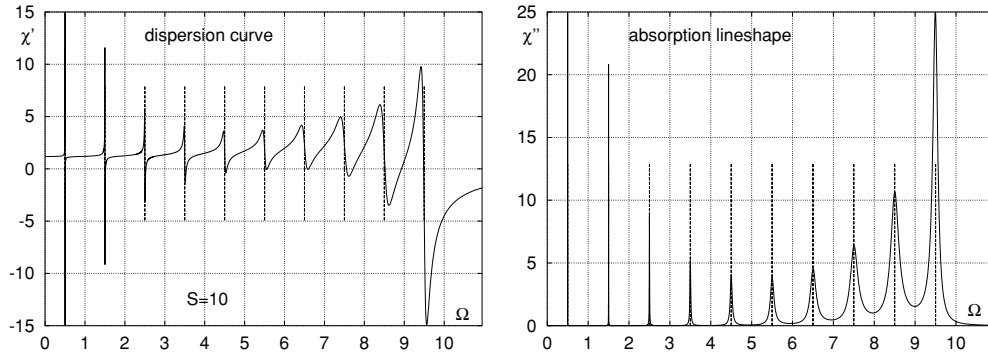
Figure 12. Continued-fraction results (lines) for $\chi_\perp(\Omega)$ of an anisotropic $S = 10$ spin with $D = 0.5$ and $\lambda/D^2 = 3 \cdot 10^{-8}$. The calculations were done at zero field and $T = 10$ ($\sigma = 5$). Real part: left panel; imaginary part: right panel. Vertical lines: loci of the transition frequencies $\Delta_{m,m+1} = D(2m+1)$, $m = 0, 1, \ldots, 9$.

$2S+1$ levels are degenerated by pairs, m with $-m$ (figure 1), and we should find only S peaks at the locations $\Omega = D(2m+1)$. The largest frequencies ($\Delta_{\rm w} \sim 2DS$) correspond to transitions at the wells ($m \sim S$), while those near the barrier top appear at low Ω ($m \sim 0$, $\Delta_{\rm b} \sim D$). Finally, as we saw in the isotropic $S = 1/2$ spin (figure 6), the absorption peaks have finite width and height due to the damping and the temperature.

Figure 12 shows these features for $S = 10$. Starting from the rightmost χ'' peak, associated with the ground-state transitions, the intensity of the peaks decreases with Ω, as they progressively involve transitions between higher levels, thermally less populated. On the other hand, the peak width is not uniform in Ω. This is due to the S_z-dependent spin–phonon interaction, $F \sim S_z S_\pm$, which gives an extra m dependence of the relaxation term (compared to the coupling $F \sim S_\pm$). This enters via the modified ladder factors $\bar{\ell}_m^2 = (2m+1)^2 \ell_m^2$ and can be seen as an effective level-dependent 'damping', $\lambda_{\rm eff}(m) \sim \lambda(2m+1)^2$. Therefore the transitions between upper levels (lower m and Ω) correspond to a reduced effective damping, and those peaks become narrower and higher. Overall, the competition of the thermal depopulation and the reduced damping yields peak heights initially decreasing as Ω is reduced and rising again at low frequencies[8].

We conclude with various effects on the line shape $\chi''(\Omega)$. The application of a field lifts the degeneracy by pairs and the peaks split (figure 13, left). At the first resonance $B_z = D$ the levels become degenerated again ($m = 0$ and $m = -1$, $m = 1$ and $m = -2, \ldots$; figure 1) and the energy differences, $\Delta = 0, 2D, 4D, \ldots$, are just halfway those of zero field, $\Delta = 1D, 3D, \ldots, D(2S-1)$. Then the 'side peak' to the right merges with that to the left of the neighbouring peak (curve not shown). For $B_z > D$ the peaks split again (they simply crossed) and at the first even resonance $B_z = 2D$ they merge again, but on the original locations (the spacings correspond to the $B_z = 0$ ones plus $\Delta = D(2S-1) + 2D$ from the ground state; figure 1). Figure 13 also shows the sharpening of the peaks when decreasing the damping (as in the isotropic $S = 1/2$ spin, with the new feature of non-uniform widths) and the dramatic reduction with temperature of the intensity of the lower Ω lines. Those transitions involve higher levels whose thermal population gets exponentially reduced as T is lowered.

---

[8] Note that $W(\Delta_{m,m\pm1})$ can also add to the dependence on m [58], except for an Ohmic bath at high T (then $W \simeq \lambda T$). However, the bare factor $\ell_m^2 = S(S+1) - m(m+1)$ does not. It is geometrical, giving the factor $(1 - z^2)$ in the classical Fokker–Planck equation [47] which accounts for the increased phase space at large angles $z = \cos\vartheta$.
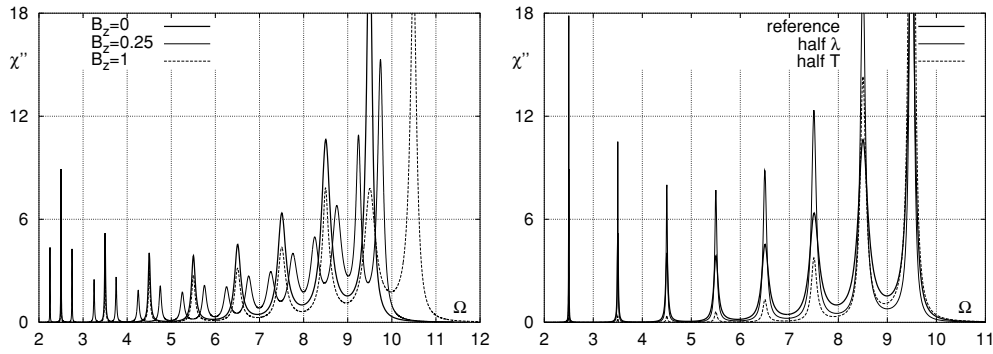
Figure 13. Effects of the external field, damping and temperature on the line shape $\chi''_\perp(\Omega)$ of anisotropic $S = 10$ spins with $D = 0.5$. Left: results for $\lambda/D^2 = 3 \cdot 10^{-8}$ and $\sigma = 5$ at $B_z = 0$ (as in figure 12), $B_z = 0.25 \,(= D/2)$ and $B_z = 1 \,(= 2D;$ cf figure 1). Right: reference zero-field line of the left together with results halving the damping at the same T, and halving T while keeping λ.

10. Summary and discussion

In the field of quantum dissipative systems one usually works with the reduced density operator ϱ of the subsystem of interest (tracing over the bath). In several problems, due to the weak system–bath coupling, one can derive perturbatively a closed equation of motion for ϱ; a quantum master equation. This plays the role of the Fokker–Planck kinetic equation in classical problems. We have addressed one such system, a quantum spin with arbitrary S in a dissipative environment, and solved exactly the corresponding density-matrix equation by implementing continued-fraction methods. As the density matrix is obtained in full, coherent dynamics is included along with the relaxation and thermoactivation.

The continued-fraction method belongs to a family of exact methods in condensed matter and statistical physics and has been fruitfully exploited in problems of Brownian motion in external potentials. Here we took advantage of the index-recurrence structure of the density-matrix equation to bring it into the form of a few-term recurrence relation, suitable to apply continued fractions. For simple spin problems this had been done by Shibata and coworkers, exploiting the decoupling into independent equations for the diagonals, $\dot{\varrho}_{m,m+k} \sim F(\varrho_{m',m'+k})$, and solving them by *scalar* continued fractions. In general such decoupling does not take place (e.g., in the presence of transverse fields), and *matrix* continued fractions are required. This has been the contribution of this work, allowing the obtainment of numerically exact solutions of the full density-matrix equation for quite generic spin problems. In addition, compared with the previous exact techniques, the affordable spin values have been increased significantly (up to $S \sim 100$–200 on an old laptop). This range of S should be enough for studying the evolution to the classical limit in many problems (one of the central issues in open quantum systems). Reaching large S is also important when effective spin models are used to describe interacting 2-level systems.

Technically, we have worked within a Hubbard formalism (Heisenberg equations of motion for the operator basis $X_n^m = |n\rangle\langle m|$), whose main advantage is being compact. This is not essential, however, and was used as an intermediate step; the equations for X_n^m are linear and their averaging gives directly the standard equations for the density-matrix elements $\varrho_{nm} = \langle n|\varrho|m\rangle$. We have focused on stationary responses, for the obtainment of which this numerical method is specially suited (in contrast with path-integral propagation schemes affected by sign problems at long times). Our starting point was to convert the time-dependent

master equation into a perturbative chain of stationary density-matrix equations with each step solvable by continued fractions. We have worked it in full for the linear dynamical susceptibility, but the extension to get non-linear responses is systematic. In addition, upon Laplace transformation, a number of time propagation problems could also be tackled (of the type 'evolution between stationary states', not 'system-meets-bath' problems requiring time-dependent coefficients).

From the outset the implementation was done in its general form (with matrix continued fractions), not taking advantage of the splitting into diagonals of simple spin problems. This made the initial tests tougher while it allowed proceeding smoothly to more general problems, not enjoying such decoupling. The implementation has been simpler than in a Fokker–Planck-type approach with pseudo-distributions, as it avoids the transformation of the density operator into some phase-space representation, the expansion in complete sets of functions, and eventually the manipulation of the coefficient recurrences (as in quantum Brownian motion in phase space). Similarly, the implementation has been easier than in the continued-fraction solution of rotational Fokker–Planck equations for *classical* spins and dipoles, as some aspects are simplified in the quantum case. For instance, the finite number of discrete levels results in *finite* continued fractions, and convergence or termination problems are fortunately bypassed. Thus, some numerical instabilities found are to be attributed to accuracy problems when handling tiny numbers; actually they appeared in parameter ranges already problematic in the classical case (very low T and Ω). On the other hand, the finite number of steps in the algorithm can be carried out by hand for small spins. The approach can actually be called semi-analytic, which is the reason behind the numerically exact agreements found with explicit solutions.

In this frame and with these tools we addressed the statics and dynamics of spins with arbitrary S in contact with a thermal bath. We have considered the familiar isotropic spin, $\mathcal{H} = -B_z S_z$, and spins in a bistable anisotropy potential $\mathcal{H} = -DS_z^2 - \boldsymbol{B} \cdot \boldsymbol{S}$ (superparamagnets). The first one, with its equispaced spectrum, is a rotational counterpart of the quantum harmonic oscillator, while the anisotropic spin corresponds to the problems of translational Brownian motion in non-harmonic potentials (double-well or periodic). The coupling to the bosonic bath considered has the structures $\mathcal{H}_{sb} \sim \boldsymbol{\eta} \cdot \boldsymbol{S}$ (bilinear) and $\mathcal{H}_{sb} \sim \{S_z, \boldsymbol{\eta} \cdot \boldsymbol{S}\}$ (non-linear). The former may describe the Kondo coupling to electron–hole excitations and the latter interaction with phonons, two important mechanisms in solids. Classically, they correspond to field-type and anisotropy-type fluctuations in the spin Langevin equations.

Both for isotropic and anisotropic spins we have given examples of static response, the dynamical susceptibility (to analyse the contribution of the different relaxation modes), and of spin resonance in transverse fields, which is very sensitive to the level spectrum and to the structure of the spin–bath coupling. Recall that effects like the spin resonance, or tunnel in transverse fields, demand the solution of the full density matrix; such coherent dynamics involves off-diagonal elements and is not captured by a Pauli balance equation for the level populations. Finally, in some examples we used parameters close to the actual quantum superparamagnets and typical experiments.

We touched in passing the issue of the validity range of a master equation description. Several limitations are inherited from the approximations required to derive quantum master equations (factorizing initial conditions, weak system–bath coupling, high-T or semiclassical bath, etc) along with manipulations specific to the problem addressed (secular or rotating-wave approximations, decoupling or adiabatic elimination of off-diagonal elements, etc). This issue, however, is independent of the question of resolvability of quantum master equations by continued fractions, a method which could in principle be applied to improved equations.

Acknowledgments

Appendix A. Energy-level spacings and effective fields

In this appendix, we calculate the level separations and related quantities (effective fields) for a uniaxial spin in a longitudinal field $\mathcal{H}_d = -DS_z^2 - B_z S_z$ (our unperturbed Hamiltonian). Then the eigenstates of S_z are eigenstates of $\mathcal{H}_d$ too, i.e., $\mathcal{H}_d|m\rangle = \varepsilon_m|m\rangle$, with $\varepsilon_m = -Dm^2 - B_z m$. The energy differences between these levels,

$$\Delta_{nm} = \varepsilon_n - \varepsilon_m \quad \rightsquigarrow \quad \Delta_{nm} = -[D(n+m) + B_z](n-m), \tag{A.1}$$

appear in the unitary part of the Heisenberg equation for the Hubbard operators (equation (5)) and control the $m \to n$ transition rate $W_{n|m} = W(\Delta_{nm})$ (equation (12)).

Level spacings. In the master equations considered, only transitions between adjacent levels enter. For $n = m \pm 1$ the energy differences (A.1) give

$$\Delta_{m,m\pm 1} = \pm[D(2m \pm 1) + B_z]. \tag{A.2}$$

In contrast with the equispaced Zeeman spectrum, the level spacings depend on m due to the anisotropy. For succesive pairs they are related by $\Delta_{m-1,m} = \Delta_{m,m+1} - 2D$, decreasing as the barrier top is approached (figure 1). To illustrate, for integer S at zero field the evolution from wells to barrier is

$$\Delta_w \equiv \Delta_{S-1,S} = D(2S-1) \to D(2S-3) \to \cdots \to 3D \to D = \Delta_{0,\pm 1} \equiv \Delta_b. \tag{A.3}$$

The boundaries coincide for $S = 1$, while $\Delta_w \sim 2DS$ for large S. For $D \sim 0.5$ K and $S = 10$ (as in Mn$_{12}$) we have the limit energy scales $\Delta_w \sim 10$ K and $\Delta_b \sim 0.5$ K. Finally, when proceeding towards the classical limit fixing the anisotropy barrier DS^2 and Zeeman energy SB, the levels approach a continuum as $\Delta \sim 1/S$.

Effective, anisotropy and critical fields. Classically one defines the effective field $B_{eff} \equiv -(\partial\mathcal{H}/\partial\mu_z)$, with $\mu_z = S\cos\vartheta$ (the spin polar angle). This quantity enters in the Landau–Lifshitz precession equation. For a Hamiltonian including only the anisotropy term $\mathcal{H} = -DS_z^2$, this definition gives the anisotropy field $B_a = 2DS\cos\vartheta$. In the quantum case the μ_z-derivative is naturally replaced by a finite difference $B_{eff} \equiv -(\varepsilon_{m+1} - \varepsilon_m)/\delta m$. Then, $\delta m = 1$ plus equation (A.2) gives the effective and anisotropy fields of the quantum problem

$$B_{eff}(m) = D(2m+1) + B_z \quad \overset{B_z=0}{\Rightarrow} \quad B_a(m) = 2D\left(m + \tfrac{1}{2}\right). \tag{A.4}$$

For $S \gg 1$, we have $B_a \simeq 2DS(m/S) \to 2DS\cos\vartheta$, recovering the classical result.

To conclude, the critical field B_c is that at which the barrier disappears (or equivalently the B_z that zeroes the last effective field $B_{eff}(-S)$; see figure 1). Equating to zero the spacing between the last two levels, $\Delta_{-S+1,-S}(B_c) = 0$, one gets

$$B_c = D(2S-1), \qquad (\simeq B_a|_{wells}). \tag{A.5}$$

This gives $B_c = 0$ for $S = 1/2$, where there is no barrier, while the classical value matches the anisotropy field at the wells, $2DS = B_a|_{\vartheta=0}$ (~ 10 T in Mn$_{12}$).
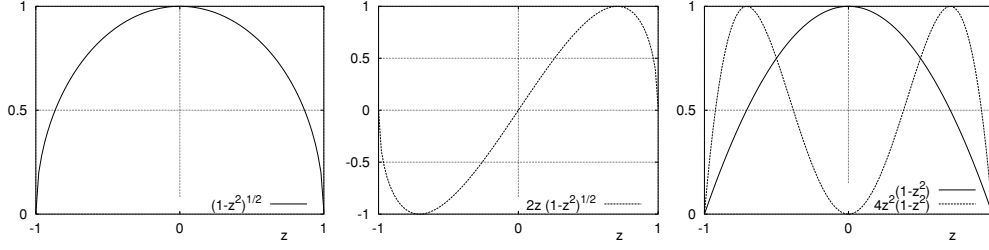
Figure 14. Functions $\ell(z) = \sqrt{1-z^2}$ and $\bar{\ell}(z) = 2z\sqrt{1-z^2}$, sketching the dependence of the ladder factors ℓ_m and $\bar{\ell}_m$ on $z \sim m/S$. Right: squared factors $\ell^2(z) = (1-z^2)$ and $\bar{\ell}^2(z) = (2z)^2(1-z^2)$, as they enter in the relaxation term.

Appendix B. Angular-momentum ladder factors

Here we discuss some properties of the ladder factors $\ell_m^\pm = [S(S+1) - m(m \pm 1)]^{1/2}$. In the standard basis of eigenstates of $\boldsymbol{S}^2$ and S_z, where $\boldsymbol{S}^2|m\rangle = S(S+1)|m\rangle$ and $S_z|m\rangle = m|m\rangle$, $\ell_m^\pm$ characterize the action of the raising/lowering operators $S_\pm|m\rangle = \ell_m^\pm|m \pm 1\rangle$. In addition they are the expansion coefficients of $S_\pm = S_x \pm iS_y$ on the Hubbard operator basis $S_\pm = \sum_m \ell_m^\pm X_{m\pm1}^m$ (equation (4)).

Ordinary factors ℓ_m. We introduce several alternative notations convenient in different contexts. The 2-index form is $\ell_{m,m'} = [S(S+1) - mm']^{1/2}$, whence

$$\ell_m^\pm = \ell_{m,m\pm1} = \sqrt{S(S+1) - m(m \pm 1)} = \ell_{m\pm1,m}. \qquad (B.1)$$

This gives an explicit index connection in the ladder action $S_\pm|m\rangle = \ell_{m,m\pm1}|m \pm 1\rangle$ as well as in $S_\pm = \sum_m \ell_{m,m\pm1} X_{m\pm1}^m$. Both $\ell_{m,m\pm1}$ can be expressed in terms of a single ladder factor ℓ_m,

$$\ell_{m,m+1} = \ell_m, \quad \ell_{m,m-1} = \ell_{m-1} \qquad \ell_m^2 = S(S+1) - m(m+1). \qquad (B.2)$$

At m and $-(m+1)$, ℓ_m take equal values: $\ell_m = \ell_{-m-1}$. Thus $\ell_S = \ell_{-S-1} = 0$ (end points), $\ell_{S-1} = \ell_{-S} = \sqrt{2S}$, $\ell_{S-2} = \ell_{-S+1} = \sqrt{2(2S-1)}, \ldots, \ell_{S-k} = \ell_{-(S+1)+k} = \sqrt{k(2S+1-k)}$. Identifying $m/S \sim z = \cos\vartheta$, we have the behaviour $\ell_m^2 \sim (1-z^2)$, which is the factor accounting for the reduction of the configuration space as the poles are approached (figure 14).

The 'bar' factors $\bar{\ell}_m$. For the spin–bath coupling $F \sim \{S_z, S_\pm\}$ we come across some modulated ladder factors in the master equation: $\bar{\ell}_{m,m\pm1} = (2m \pm 1)\ell_{m,m\pm1}$. Using $2m \pm 1 = m + (m \pm 1)$ we can write in a symmetric way

$$\bar{\ell}_{m,m'} = \bar{\ell}_{m',m} = (m + m')\ell_{m,m'}. \qquad (B.3)$$

Again we can introduce a compact single factor $\bar{\ell}_m$:

$$\bar{\ell}_{m,m+1} = \bar{\ell}_m, \quad \bar{\ell}_{m,m-1} = \bar{\ell}_{m-1}, \qquad \bar{\ell}_m \equiv (2m+1)\ell_m. \qquad (B.4)$$

The symmetry $\ell_{-m} = \ell_{m-1}$, together with $(-2m+1) = -(2m-1)$, yields the corresponding (anti)symmetry of the bar factors, namely $\bar{\ell}_{-m} = -\bar{\ell}_{m-1}$. Then $\bar{\ell}_S = -\bar{\ell}_{-S-1} = 0$ (boundaries), $\bar{\ell}_{S-1} = -\bar{\ell}_{-S} = (2S-1)\sqrt{2S}$, $\bar{\ell}_{S-2} = -\bar{\ell}_{-S+1} = (2S-3)\sqrt{2(2S-1)}, \ldots, \bar{\ell}_{S-k} = \bar{\ell}_{-(S+1)+k} = (2S+1-2k)\sqrt{k(2S+1-k)}$.

For half-integer spin, $\bar{\ell}_m$ vanishes at $m = -1/2$. In general $\bar{\ell}_m$ goes close to zero for small m (barrier top) as it has opposite signs for positive and negative m (figure 14, middle). For $S = 1/2$ all relevant $\bar{\ell}_m$ vanish, reflecting that the coupling $F \sim \{S_z, S_\pm\}$ does not produce

relaxation on a $S = 1/2$ spin; physically, this F arises from the modulation of the anisotropy $-DS_z^2$ by the lattice vibrations [32], but S_z^2 does not change the energy of $S = 1/2$ (recall the equilibrium result $m_z = \frac{1}{2} \operatorname{th}\left(\frac{1}{2} B_z / T\right)$).

Appendix C. The Hubbard (level-shift) operators

In this appendix, we discuss some properties of operators $X_n^m = |n\rangle\langle m|$ and derive their Heisenberg equations of motion in the conservative case. They form a complete set; if we think of a spin operator as a $(2S + 1) \times (2S + 1)$ matrix, then X_n^m is the matrix with zeros everywhere, except a 1 at the position (n, m) [35, chapter 1]. In this space of linear operators, they form an orthonormal system with respect to the scalar product $(X, Y) \equiv \operatorname{Tr}(X^+ Y)$.

Properties of X_n^m. We begin by demonstrating several useful results.

- *Expressing an operator A in the Hubbard basis*

$$A = \sum_{nm} A_{nm} X_n^m, \qquad A_{nm} = \langle n|A|m\rangle. \tag{C.1}$$

Proof. Using twice the closure relation $I = \sum_m |m\rangle\langle m|$,

$$A = \sum_n |n\rangle\langle n|A \sum_m |m\rangle\langle m| = \sum_{nm} \langle n|A|m\rangle|n\rangle\langle m| = \sum_{nm} A_{nm} X_n^m.$$
$\square$

- *Equal-time relation*

$$X_n^k X_l^m = \delta_{kl} X_n^m. \tag{C.2}$$

Proof. Using the $|m\rangle$ basis orthonormality, $X_n^k X_l^m = |n\rangle\langle k|l\rangle\langle m| = \delta_{kl} X_n^m.$ $\square$

- *Commutator*

$$\left[X_n^k, X_l^m\right] = \delta_{kl} X_n^m - \delta_{nm} X_l^k. \tag{C.3}$$

Proof. $\left[X_n^k, X_l^m\right] = X_n^k X_l^m - X_l^m X_n^k$ plus the equal-time relation (C.2). $\square$

- *Adjoint* (recall the zeros plus 1 at (n, m) representation of X_n^m)

$$\left(X_n^m\right)^+ = X_m^n. \tag{C.4}$$

Proof. We use the auxiliary notation $\langle\psi, \phi\rangle$ for the scalar product:

$$\langle(X_n^m)^+\psi, \phi\rangle = \langle\psi, X_n^m\phi\rangle = \langle\psi|n\rangle\langle m|\phi\rangle = \left(\langle\phi|m\rangle\langle n|\psi\rangle\right)^* = \langle\phi, X_m^n\psi\rangle^* = \langle X_m^n\psi, \phi\rangle.$$

The validity of this result $\forall\psi$ and ϕ gives equation (C.4). $\square$

- *Relation with the density matrix* (note the index ordering)

$$\langle X_n^m\rangle = \varrho_{mn}. \tag{C.5}$$

Proof. Use the level-shift property $X_n^m|k\rangle = \delta_{mk}|n\rangle$ and $\langle A\rangle \equiv \operatorname{Tr}(\varrho A)$:

$$\operatorname{Tr}\left(\varrho X_n^m\right) = \sum_k \langle k|\varrho X_n^m|k\rangle = \sum_k \langle k|\varrho|n\rangle\delta_{mk} = \varrho_{mn}.$$

As corollaries, replacing $\varrho \to I$ one gets the *trace formula* $\mathrm{Tr}\left(X_n^m\right) = \delta_{nm}$. Then one can prove the orthonormality of the Hubbard basis: $\left(X_n^m, X_k^l\right) \equiv \mathrm{Tr}\left[\left(X_n^m\right)^+ X_k^l\right] = \mathrm{Tr}\left(X_m^n X_k^l\right) = \mathrm{Tr}\left(\delta_{nk} X_m^l\right) = \delta_{nk}\delta_{ml}$. □

Heisenberg equation of motion. As the Hubbard operators X_n^m do not depend explicitly on t, their Heisenberg dynamical equation is simply $i\dot{X}_n^m = \left[X_n^m, \mathcal{H}\right]$. Here we derive it explicitly for a Hamiltonian comprising a diagonal part $\mathcal{H}_d(S_z)$ (in the standard basis) plus a transverse field: $\mathcal{H} = \mathcal{H}_d(S_z) - \frac{1}{2}(B_+ S_- + B_- S_+)$.

Let us commute the different parts of $\mathcal{H}$ with X_n^m. For $\mathcal{H}_d$ we can write $\mathcal{H}_d = \sum_k \varepsilon_k X_k^k$, since its matrix elements are $\langle n|\mathcal{H}_d|m\rangle = \varepsilon_m \delta_{nm}$ (see equation (C.1)). Then, we work $\left[X_n^m, \mathcal{H}_d\right]$ out with the help of equation (C.3),

$$\left[X_n^m, \mathcal{H}_d\right] = \sum_k \varepsilon_k\left[X_n^m, X_k^k\right] = \sum_k \varepsilon_k\left(\delta_{mk} X_n^k - \delta_{kn} X_k^m\right) = -\Delta_{nm} X_n^m,$$

where $\Delta_{nm} = \varepsilon_n - \varepsilon_m$. For the transverse components we employ the representation $S_\pm = \sum_k \ell_{k,k\pm 1} X_{k\pm 1}^k$ (equation (4)) and again commutator (C.3),

$$\left[X_n^m, S_\pm\right] = \sum_k \ell_{k,k\pm 1}\left[X_n^m, X_{k\pm 1}^k\right] = \sum_k \ell_{k,k\pm 1}\left(\delta_{m,k\pm 1} X_n^k - \delta_{n,k} X_{k\pm 1}^m\right)$$

$$= \ell_{m\mp 1,m} X_n^{m\mp 1} - \ell_{n,n\pm 1} X_{n\pm 1}^m = \ell_m^\mp X_n^{m\mp 1} - \ell_n^\pm X_{n\pm 1}^m,$$

where we have used $\ell_{m,m'} = \ell_{m',m}$ and $\ell_{m,m\pm 1} = \ell_m^\pm$ (appendix B). Finally gathering these partial results, including $-B_\pm/2$, and multiplying across by $-i$,

$$\dot{X}_n^m = -i\left[X_n^m, \mathcal{H}_d\right] + (i/2)B_+\left[X_n^m, S_-\right] + (i/2)B_-\left[X_n^m, S_+\right],$$

we arrive at the unitary evolution equation (5) for the Hubbard operators.

A final comment. If we had used the exact eigenstates of the total Hamiltonian, the term $i\Delta_{nm} X_n^m$ would have been the only term in the equation (with $B_\pm$ entering via ε_m). Using the angular-momentum basis instead (for example, when the exact eigenstructure is not known or, for convenience, to treat time-dependent $B_\pm$), one needs to add explicitly the contribution of the transverse terms, as we have done here.

Appendix D. The relaxation term

In contact with the bath the closed equation of motion (5) is augmented by the relaxation term (9). Here starting from such R_n^m we derive the time-local relaxation term (11) and then we particularize it to spin–bath couplings via $S_\pm$. Finally, we discuss the adoption of the secular or rotating-wave approximation and the issue of the positivity of the reduced description.

D.1. Derivation of the time-local relaxation term (11)

We start from $-R_n^m = \int_{-\infty}^t d\tau\left\{\mathcal{K}(\tau - t)F(\tau)\left[F, X_n^m\right] - \mathcal{K}(t - \tau)\left[F, X_n^m\right]F(\tau)\right\}$, where operators without argument are evaluated at t. The formal dependence on the previous evolution enters through $F(\tau)$. We expand it on the Hubbard basis, $F(\tau) = \sum_{kl} F_{kl} X_k^l(\tau)$, and replace the retarded dependences by the (dominant) S_z-part of the conservative evolution $X_k^l(\tau) = e^{-i(t-\tau)\Delta_{kl}} X_k^l(t)$, whence $F(\tau) = \sum_{kl} F_{kl} e^{-i(t-\tau)\Delta_{kl}} X_k^l(t)$. Next, the change of variable $s = t - \tau$ brings the integral relaxation term into the form

$$-R_n^m = \sum_{kl} F_{kl} \int_0^\infty ds\left\{\mathcal{K}(-s) e^{-is\Delta_{kl}} X_k^l\left[F, X_n^m\right] - \mathcal{K}(s) e^{-is\Delta_{kl}}\left[F, X_n^m\right]X_k^l\right\}.$$

The s-dependences only occur in kernel and in the oscillating factors. Integrating them brings into the scene the relaxation rates $W_{k|l} = W(\Delta_{kl})$, with $W(\Delta) = \int_0^\infty ds\, e^{-is\Delta}\mathcal{K}(s)$

(equation (12)). Then, using $\mathcal{K}(-\tau) = [\mathcal{K}(\tau)]^*$ and $\Delta_{lk} = -\Delta_{kl}$ gives

$$-R_n^m = \sum_{kl} F_{kl} \{ W_{l|k}^* X_k^l [F, X_n^m] - W_{k|l} [F, X_n^m] X_k^l \}. \tag{D.1}$$

This completes the task of getting a time-local relaxation term. Note however that R_n^m still depends on X in a non-explicit way (since F also contains them)[9].

The rest of the calculation consists of simplifying the X structure of the above term. First, we expand the inner F as $F = \sum_{k'l'} F_{k'l'} X_{k'}^{l'}$ and use $[X_{k'}^{l'}, X_n^m] = \delta_{nl'} X_{k'}^m - \delta_{mk'} X_n^{l'}$ to work the commutators. Then we multiply by X_k^l (from the left and right) and use the equal-time relation $X_k^l X_n^m = \delta_{ln} X_k^m$ to get expressions linear in the Hubbard basis. Eventually, the result of the left and right multiplications is in turn multiplied by $W_{l|k}^* F_{kl}$ and $W_{k|l} F_{kl}$ respectively (equation (D.1)) and summed over k and l:

$$\sum_{kl} W_{l|k}^* F_{kl} X_k^l [F, X_n^m] = \sum_{kl} W_{l|k}^* F_{kl} F_{ln} X_k^m - \sum_{kl'} W_{n|k}^* F_{kn} F_{ml'} X_k^{l'}$$

$$\sum_{kl} W_{k|l} F_{kl} [F, X_n^m] X_k^l = \sum_{lk'} W_{m|l} F_{ml} F_{k'n} X_{k'}^l - \sum_{kl} W_{k|l} F_{kl} F_{mk} X_n^l.$$

To clarify the structure and to arrive at the sought form $\sum_{n'm'} \mathcal{W}_{n,n'}^{m,m'} X_{n'}^{m'}$ we make several index changes. First line, first term: $l \to \ell$ (summed index), $k \to n'$, and we introduce $\sum_{m'} \delta_{mm'}$. First line, second term: $l' \to m'$ and $k \to n'$. Second line, first term: $k' \to n'$ and $l \to m'$. Second line, second term: $k \to \ell$ (summed index), $l \to m'$, and introduce $\sum_{n'} \delta_{nn'}$. Then we obtain for the above right-hand sides

$$\sum_{n'm'} \left[\delta_{mm'} \sum_{\ell} W_{\ell|n'}^* F_{n'\ell} F_{\ell n} - W_{n|n'}^* F_{n'n} F_{mm'} \right] X_{n'}^{m'}$$

$$\sum_{n'm'} \left[W_{m|m'} F_{mm'} F_{n'n} - \delta_{nn'} \sum_{\ell} W_{\ell|m'} F_{\ell m'} F_{m\ell} \right] X_{n'}^{m'}.$$

Substraction of these lines according to equation (D.1) gives finally the relaxation term (11).

D.2. Relaxation term for couplings via $S_\pm$

Here we particularize the relaxation term (11) to the coupling (13), with $F(\mathbf{S})$ 'linear' in $S_\pm$. We start expanding the anticommutators and introducing $F_\pm = \eta_\mp [v(S_z) S_\pm + S_\pm v(S_z)]$, so that $F = F_- + F_+$. To obtain the matrix elements $F_{nm} = \langle n|F|m \rangle$ we compute first those of F_-, using $S_-|m\rangle = \ell_{m,m-1}|m-1\rangle$:

$$(F_-)_{nm} = L_{m,m-1} \delta_{n,m-1}, \qquad L_{m,m'} = \eta_+ [v(m) + v(m')] \ell_{m,m'}. \tag{D.2}$$

Note that the extended ladder factor $L_{m,m'}$ is in general complex. Then by means of $F_+ = (F_-)^+$ we arrive at $F_{nm} = L_{m,m-1} \delta_{n,m-1} + L_{m+1,m}^* \delta_{n,m+1}$ (i.e., equation (14)).

Let us proceed to do the sums in the relaxation term (11) with these matrix elements and some care. For the *third line* we need $\sum_{\ell m'} W_{\ell|m'} F_{m\ell} F_{\ell m'} X_n^{m'}$. The sum over m' gives

$$\sum_{m'} W_{\ell|m'} F_{\ell m'} X_n^{m'} = L_{\ell+1,\ell} W_{\ell|\ell+1} X_n^{\ell+1} + L_{\ell,\ell-1}^* W_{\ell|\ell-1} X_n^{\ell-1}.$$

---

[9] It is assumed that at the initial time, $t_0 = -\infty$, system and bath were decoupled. If this is assumed to occur at some finite t_0, the rates acquire a time dependence $W(\Delta; t) = \int_0^{t-t_0} \mathrm{d}s\, \mathrm{e}^{-\mathrm{i}s\Delta} \mathcal{K}(s)$. However, as in most problems system and bath had coexisted for a very long time, one shifts $t_0 \to -\infty$ and the transients due to such decoupled initial conditions are washed away.

Multiplying by $F_{m\ell} = L_{m+1,m}\delta_{\ell,m+1} + L^*_{m,m-1}\delta_{\ell,m-1}$ and summing over ℓ we obtain

$$
\begin{aligned}
\text{third line} = {} & L^*_{m,m-1}L^*_{m-1,m-2}W_{m-1|m-2}X_n^{m-2} \\
& + (|L_{m,m-1}|^2 W_{m-1|m} + |L_{m+1,m}|^2 W_{m+1|m})X_n^m \\
& + L_{m+2,m+1}L_{m+1,m}W_{m+1|m+2}X_n^{m+2}.
\end{aligned}
$$

The perturbative paths are clear, e.g., $m+2 \to m+1 \to m$ to connect X_n^{m+2} with X_n^m. Inspection of equation (11) reveals that the *first line* follows from the third by exchanging $m \leftrightarrow n$, conjugating, and permuting upper and lower indices in X (adjoining):

$$
\begin{aligned}
\text{first line} = {} & L_{n,n-1}L_{n-1,n-2}W^*_{n-1|n-2}X_{n-2}^m \\
& + (|L_{n,n-1}|^2 W^*_{n-1|n} + |L_{n+1,n}|^2 W^*_{n+1|n})X_n^m \\
& + L^*_{n+2,n+1}L^*_{n+1,n}W^*_{n+1|n+2}X_{n+2}^m.
\end{aligned}
$$

Now we are left with $\sum_{n'm'}(W^*_{n|n'} + W_{m|m'})F_{n'n}F_{mm'}X_{n'}^{m'}$, the central line of equation (11). Exclude $F_{n'n}$ and do first the sum over m', then multiply by $F_{n'n}$ written in the form $F_{n'n} = L_{n,n-1}\delta_{n',n-1} + L^*_{n+1,n}\delta_{n',n+1}$, sum over n', and reverse signs; you should get

$$
\begin{aligned}
\text{second line} = {} & -L_{n,n-1}L^*_{m,m-1}(W^*_{n|n-1} + W_{m|m-1})X_{n-1}^{m-1} \\
& - L^*_{n+1,n}L^*_{m,m-1}(W^*_{n|n+1} + W_{m|m-1})X_{n+1}^{m-1} \\
& - L_{n,n-1}L_{m+1,m}(W^*_{n|n-1} + W_{m|m+1})X_{n-1}^{m+1} \\
& - L^*_{n+1,n}L_{m+1,m}(W^*_{n|n+1} + W_{m|m+1})X_{n+1}^{m+1}.
\end{aligned}
$$

Collecting the three contributions we finally obtain the specialization of the Markovian relaxation term (11) to the coupling (13):

$$
\begin{aligned}
R_n^m = {} & L_{n,n-1}L^*_{m,m-1}(W^*_{n|n-1} + W_{m|m-1})X_{n-1}^{m-1} \\
& - (|L_{n+1,n}|^2 W^*_{n+1|n} + |L_{m+1,m}|^2 W_{m+1|m} \\
& + |L_{n,n-1}|^2 W^*_{n-1|n} + |L_{m,m-1}|^2 W_{m-1|m})X_n^m \\
& + L^*_{n+1,n}L_{m+1,m}(W^*_{n|n+1} + W_{m|m+1})X_{n+1}^{m+1} \\
& - L_{n,n-1}L_{n-1,n-2}W^*_{n-1|n-2}X_{n-2}^m - L^*_{n+2,n+1}L^*_{n+1,n}W^*_{n+1|n+2}X_{n+2}^m \qquad \leftarrow \\
& + L_{n,n-1}L_{m+1,m}(W^*_{n|n-1} + W_{m|m+1})X_{n-1}^{m+1} \\
& + L^*_{n+1,n}L^*_{m,m-1}(W^*_{n|n+1} + W_{m|m-1})X_{n+1}^{m-1} \\
& - L^*_{m,m-1}L^*_{m-1,m-2}W_{m-1|m-2}X_n^{m-2} - L_{m+2,m+1}L_{m+1,m}W_{m+1|m+2}X_n^{m+2}. \quad \text{(D.3)}
\end{aligned}
$$

On invoking the secular approximation (see below) terms involving $L \times L$ or $L^* \times L^*$ are dropped (last four lines) and only the terms of the type $L \times L^*$ are retained (first four). This gives the secularized relaxation term (15) in the main text.

D.3. The non-secular terms and the positivity issue

Neglecting the 'non-secular' terms $L \times L$ and $L^* \times L^*$ corresponds to the rotating-wave approximation of quantum optics, where counterrotating terms are dropped. Specifically, writing schematically the coupling as $\mathcal{H}_{sb} \sim S_-(a^+ + \epsilon a) + S_+(a + \epsilon a^+)$, one can see that setting $\epsilon = 0$ the last four lines of equation (D.3) disappear [43]. To justify this manipulation, it is argued that $a^+ S_+ \sim e^{i(\omega+\Delta)t}$ oscillates faster than $a^+ S_- \sim e^{i(\omega-\Delta)t}$ and can be averaged out. A word of caution though. While this reasoning may apply to systems with a monotonous spectrum (harmonic oscillator, isotropic spin), the justification is not satisfactory if the sign of

$\Delta_{m,m+1}$ depends on m (upon $\Delta \to -\Delta$ it would be a^+S_-, the term oscillating fast, and a^+S_+, which is dropped, the slow one).

Keeping all terms in equation (D.3) does not pose big problems for a continued-fraction solution. Only the line marked with the arrow (fifth one) breaks the 3-term recurrence in n, giving $\dot{c}_n \sim \mathbb{Q}_{n,n-2}c_{n-2} + \mathbb{Q}_{n,n-1}c_{n-1} + \mathbb{Q}_{n,n}c_n + \mathbb{Q}_{n,n+1}c_{n+1} + \mathbb{Q}_{n,n+2}c_{n+2}$, as the equation of motion for $(c_n)_m = \langle X_n^m \rangle$. But this can be treated by $5 \to 3$ recurrence folding with block vectors and matrices [4, 20]

$$\mathbf{C}_n = \begin{pmatrix} c_{2n} \\ c_{2n+1} \end{pmatrix} \qquad \mathbf{Q}_{n,n'} = \begin{pmatrix} \mathbb{Q}_{2n,2n'} & \mathbb{Q}_{2n+1,2n'} \\ \mathbb{Q}_{2n,2n'+1} & \mathbb{Q}_{2n+1,2n'+1} \end{pmatrix},$$

recovering the canonical form $\dot{\mathbf{C}}_n \sim \mathbf{Q}_{n,n-1}\mathbf{C}_{n-1} + \mathbf{Q}_{n,n}\mathbf{C}_n + \mathbf{Q}_{n,n+1}\mathbf{C}_{n+1}$. Alternatively, one can handle $c_{n\pm2}$ in an iterative way (keeping the ordinary vectors and matrices) which converges quickly for weak damping. Notwithstanding this, we preferred to illustrate the continued-fraction treatment of the master equation with a simple yet generic case.

Incidentally, the density-matrix equation without non-secular terms is of the so-called Lindblad type [62] for isotropic spins. In general, however, equation (D.3) does not ensure that, for arbitrary initial conditions, ϱ is a positive operator at all times (which is required for its probabilistic interpretation). Although this sounds alarming, no real problem exists when one recalls the assumptions under which the master equation is derived and the meaning of ϱ as partial trace of ϱ_{tot}.

First, to derive the master equation one assumes that at some initial time t_0 system and bath were decoupled $\varrho_{\mathrm{tot}}(t_0) = \varrho(t_0) \otimes \varrho_{\mathrm{b}}(t_0)$. The resulting evolution equation for $\varrho = \mathrm{Tr}_{\mathrm{b}}(\varrho_{\mathrm{tot}})$ is precisely equation (D.3) but with some time-dependent coefficients (recall footnote 9 above). But as this master equation comes from the solution of $\mathrm{i}(\mathrm{d}\varrho_{\mathrm{tot}}/\mathrm{d}t) = [\mathcal{H}, \varrho_{\mathrm{tot}}]$, which preserves positivity of ϱ_{tot} (and hence of any partial trace), then $\varrho(t) > 0$ should hold to the accuracy considered in the system–bath coupling. Actually, no positivity violation has been reported when using the proper time-dependent coefficients. The cases of $\varrho < 0$ explicitly shown [63, 64] correspond to the use of the master equation with the asymptotic t-independent coefficients (valid at long times), to address arbitrary initial condition problems. However, in the asymptotic regime, system and bath have been interacting for a long time and the possible $\varrho(t = 0) = \mathrm{Tr}_{\mathrm{b}}(\varrho_{\mathrm{tot}})$ cannot be chosen at our will.

Except in problems like the atom inserted in an electromagnetic cavity or the like, decoupled initial conditions are just a mathematical trick to facilitate obtaining the form of the master equation. For problems like a spin in a solid, a Brownian particle in a fluid etc, it is not reasonable to assume that system and bath just met, but that they were in contact for a long time. Thus, one shifts the initial time $t_0 \to -\infty$, so that at finite times (say $t \geqslant 0$) those factorizing initial conditions have been forgotten (except maybe in marginal cases) and system-plus-bath have evolved into some joint stationary state by their internal dynamics. Then the coefficients to be used are the asymptotic ones. But then it is natural that the initial conditions for $\varrho(t = 0)$ cannot be set arbitrarily, but only those compatible with the evolution of the coupled system-plus-bath. It is only overlooking this point that the positivity becomes a issue.

Finally, in the asymptotic $t \geqslant 0$ regime, one can manipulate the system with fields or forces to prepare 'initial conditions' for the problems of interest. This will only result in some time dependences of the master equation coefficients. In our case they arise when evolving $X(s)$ back in time in the memory kernel, which now has to be done as $X(s) = X(t)\exp\left[-\mathrm{i}\int_t^s \mathrm{d}u\,\Delta(u)\right]$, with the proper time-dependent Hamiltonian evolution [41]. If the manipulation of the system is slow compared to the kernel width (bath correlation time), one can use the leading term $X(s) \simeq X(t)\,\mathrm{e}^{-\mathrm{i}(s-t)\Delta(t)}$. Then one obtains precisely
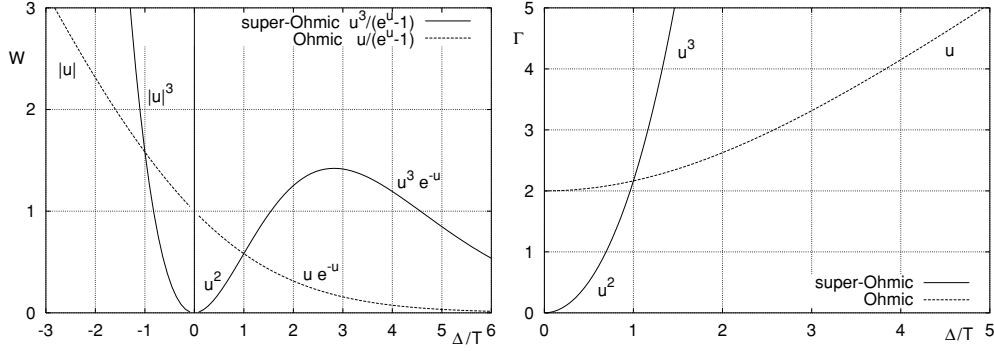
Figure 15. Transition rate $W(u)$ (left panel) and relaxation rate $\Gamma = W(u) + W(-u)$ (right). Curves for both the Ohmic bath, $J(\omega) \propto \omega$ (dashed lines), and the super-Ohmic bath $J(\omega) \propto \omega^3$ (solid) are shown. The limit functional dependences on $u = \Delta/T$ are marked. Introducing a high-frequency cut-off ω_D in $J(\omega)$, both $W(u)$ and $\Gamma(u)$ would eventually drop to zero for $|u| \gg \omega_D/T$, reflecting that no quanta of arbitrary large ω are available to interchange energy with.

the ordinary master equation, with the asymptotic form of the coefficients, but parametrically modulated by the time-dependent fields or forces.

Preparing the system in this way, the initial conditions follow from the master equation dynamics (and there is a single continuous process from $t_0 = -\infty$, instead of the 'initial conditions' being set twice). Then, to the accuracy in the coupling considered, the positivity, hermiticity, normalization, etc, are preserved inasmuch as $i(d\varrho_{tot}/dt) = [\mathcal{H}, \varrho_{tot}]$ underlies the reduced dynamics for $\varrho = \mathrm{Tr}_b(\varrho_{tot})$.

Appendix E. Transition and relaxation rates

The rate function $W(\Delta)$, associated with the kernel $\mathcal{K}(\tau)$, can be expressed in terms of the bath spectral density (equation (16)). This follows integrating relation (10) between $\mathcal{K}(\tau)$ and $J(\omega)$ with $\mathrm{Re}\left[\int_0^\infty d\tau \exp(-i\tau\Delta)\right] = \pi\delta(\Delta)$. In this appendix, we consider $W(\Delta)$ for spectral densities of the form $J(\omega) = \lambda\omega^\alpha$. We address two cases: (i) Ohmic bath $\alpha = 1$ and (ii) the custom $\alpha = 3$ super-Ohmic bath (photons or phonons in three dimensions). Note that in both cases α is odd.

Unified functional form. Introducing the reduced variable $u = \Delta/T$ and omitting proportionality constants we write equation (16) as $W(u > 0) = u^\alpha n_u$ and $W(u < 0) = |u|^\alpha(n_{|u|} + 1)$ with the Bose factor $n_u = 1/(e^u - 1)$. Let us first demonstrate that a single functional form gives the rates for both $u < 0$ and $u > 0$:

$$W(-u) \overset{u \geq 0}{=} |-u|^\alpha(n_{|-u|} + 1) = u^\alpha\left(\frac{1}{e^u - 1} + 1\right) = \frac{u^\alpha}{1 - e^{-u}} = \frac{(-u)^\alpha}{e^{-u} - 1}.$$

Note that we have used the oddness of the spectral index α to absorb the sign change of the denominator (otherwise a $\mathrm{sgn}(u)$ appears). Thus $W(-u)$ has the same functional dependence as the positive u case, i.e., $(-u)^\alpha n_{-u}$, and we can write

$$J(\omega) \propto \omega^\alpha \text{ (odd } \alpha) \quad \rightsquigarrow \quad W(u) = \frac{u^\alpha}{e^u - 1}, \quad \forall u. \tag{E.1}$$

Figure 15 displays the dependences of W on $u = \Delta/T$ for $\alpha = 1$ and 3. For large and negative

energy differences (emission of quanta) the behaviour is $|u|^\alpha$. In the Ohmic case, the rate decreases monotonically from $W(0) = 1$ for positive energy differences (absorption). The super-Ohmic $W(u)$, in contrast, after an initial parabolic takeoff from zero, has a maximum at $u \sim 2\sqrt{2}$ and decreases exponentially dominated for large energy absorption.

Derivatives of $W(u)$. These are needed in the perturbative calculations (section 7.2). Having the unified functional form (E.1) we can differentiate without worrying about distinguishing between absorption and emission processes:

$$W'(u) = \frac{\alpha u^{\alpha-1}}{e^u - 1} + \frac{u^\alpha}{(e^u - 1)(e^{-u} - 1)}. \tag{E.2}$$

In the perturbative treatment of the probing field we actually need the B_z-derivatives of $W_{m|m\pm1}$. Applying the chain rule $\mathrm{d}W/\mathrm{d}B_z = W'(u)\mathrm{d}u/\mathrm{d}B_z$ we obtain a $\pm$ sign depending on the transition 'lowering' or 'raising' the second index (see equation (A.2)):

$$W_{m|m\pm1} \sim \Delta_{m,m\pm1} = \pm[D(2m \pm 1) + B_z] \quad \rightsquigarrow \quad \partial_{B_z}\Delta_{m,m\pm1} = \pm1.$$

Finally, one must recall to multiply equation (E.2) also by $1/T$ since $u = \Delta/T$.

Relaxation rate. The combination $\Gamma(u) = W(u) + W(-u)$ occurs in several problems (isotropic $S = 1/2$ and $S = 1$ spins, section 8.3.1, anisotropic $S = 1$, section 9.3.1). Using equation (E.1) this symmetrized rate can be written as

$$\Gamma \equiv W(u) + W(-u) = u^\alpha \operatorname{cth}\left(\tfrac{1}{2}u\right). \tag{E.3}$$

This function behaves as $2u^{\alpha-1}$ for small u then grows monotonically and for large energy differences goes as u^α (figure 15, right). The monotony is proved by differentiating equation (E.3), whence $\Gamma' = \tfrac{1}{2}u^{\alpha-1}(\alpha \operatorname{sh} u - u)/\operatorname{sh}^2\left(\tfrac{1}{2}u\right) > 0$, for $\alpha \geqslant 1$.

Appendix F. Integral relaxation time

The advantage of this quantity is that it can be obtained from the low-frequency response $\chi(\Omega) \simeq \chi(1 - \mathrm{i}\Omega\tau_{\mathrm{int}} + \ldots)$. This result follows from the definition $\tau_{\mathrm{int}} \equiv \int_0^\infty \mathrm{d}t\, \delta M(t)/\delta M(0)$ plus a low Ω expansion in the linear-response-theory relation $\chi(\Omega) = \chi\left(1 - \mathrm{i}\Omega \int_0^\infty \mathrm{d}t\, e^{-\mathrm{i}\Omega t}[\delta M(t)/\delta M(0)]\right)$. Here we discuss a generalization of the results for τ_{int} of [31, 32, 44] by considering a generic discrete system obeying balance equations of the form [47]

$$\dot{N}_m = (P_{m|m-1}N_{m-1} - P_{m-1|m}N_m) + (P_{m|m+1}N_{m+1} - P_{m+1|m}N_m). \tag{F.1}$$

Here $P_{m|m'}$ is the $m' \to m$ transition probability, assumed to depend on the level spacings $P_{m|m'} = P(\Delta_{mm'})$ and to obey detailed balance $P_{m|m'} = e^{-\Delta_{mm'}/T}P_{m'|m}$. In addition, the level separation is controlled by some bias F as $\Delta = \Delta^{(0)} + F$.

Next one augments F by an oscillating probe $F \to F + \tfrac{1}{2}f\, e^{\mathrm{i}\Omega t} + \mathrm{c.c.}$ and seeks for a solution of equation (F.1) of the form $N_m = N_m^{(0)} + \tfrac{1}{2}f\left(N_m^{(1)}\, e^{\mathrm{i}\Omega t} + \mathrm{c.c.}\right)$. The corresponding susceptibility is $\chi(\Omega) \sim \sum_m m N_m^{(1)}(\Omega)$. At low frequencies the equations for $N_m^{(1)}$ can be solved analytically and one gets $\chi(\Omega \to 0)$, whence τ_{int} follows as [47, appendix B]

$$\tau_{\mathrm{int}} = \frac{1}{M'}\sum_m \frac{\Phi_m^2}{N_m^{(0)} P_{m+1|m}^{(0)}}, \qquad \Phi_m = \sum_{k=m_\mathrm{i}}^m N_k^{(0)}(M - k). \tag{F.2}$$

Here $M' = \mathrm{d}M/\mathrm{d}y$, with $y = F/T$ and $M = \sum_m m N_m^{(0)}$ is the static response. The range of m is $[m_\mathrm{i}, m_\mathrm{f}]$ and the superscript (0) indicates the absence of the probing field. Note that the auxiliary function Φ_m, in contrast to $P_{m|m'}$, depends only on equilibrium properties.

To get τ_{int} for isotropic spins, we simply cast the corresponding balance equations (section 5.1) into the form (F.1), by identifying $P_{m|m'} = \ell_{m,m'}^2 W_{m|m'}$. To do so we have taken advantage of the 2-index form (B.1) of the ladder coefficients ($\ell_{m-1} = \ell_{m,m-1} = \ell_{m-1,m}$, and $\ell_m = \ell_{m,m+1} = \ell_{m+1,m}$), and recalled the simplified relations $W_{m|m-1} = w_0$ and $W_{m-1|m} = w_0 \, e^{-y}$ (section 5.1). Thus τ_{int} in this case is given by $\tau_{\text{int}} = (1/m_z') \sum_{m=-S}^{S} \left(\Phi_m^2 / N_m^{(0)} \ell_m^2 w_0 \right)$, with $\Phi_m = \sum_{k=-S}^{m} N_k^{(0)} (m_z - k)$ [31].

To obtain τ_{int} for anisotropic spins we similarly bring their balance equations into the above form (section 9.3.1). We use the 2-index notation of the modified factors $\bar{\ell}_m = \bar{\ell}_{m,m+1}$ and $\bar{\ell}_{m-1} = \bar{\ell}_{m,m-1}$ plus $\bar{\ell}_{m,m'} = \bar{\ell}_{m',m}$ (equation (B.3)) and identify $P_{m|m'} = \bar{\ell}_{m,m'}^2 W_{m|m'}$. Then the generic expression (F.2) gives the relaxation time of the anisotropic-spin problem as $\tau_{\text{int}} = (1/m_z') \sum_m \left(\Phi_m^2 / N_m^{(0)} \bar{\ell}_m^2 W_{m+1|m}^{(0)} \right)$, with the same expression for Φ_m (cf equation (5.13) in [32] and equation (16) in [44]). Recall finally that, in contrast to the isotropic case, no simplification occurs in the rates $W_{m+1|m}$ because of the non-equispaced spectrum.

Appendix G. Continued-fraction methods to solve recurrence relations

We conclude with a hands-on summary of the method of resolution of 3-term recurrences of the form

$$Q_i^- C_{i-1} + Q_i C_i + Q_i^+ C_{i+1} = -f_i, \qquad i = 1, 2, 3, \ldots \tag{G.1}$$

Here Q_i are given coefficients ($Q_1^- \equiv 0$) and f_i are forcing or source terms. To obtain the unknown C_i one inserts in equation (G.1) the ansatz [4, 14, 16]

$$C_i = S_i C_{i-1} + a_i, \tag{G.2}$$

obtaining the following relations for the ladder coefficients S_i and shifts a_i:

$$S_i = -\frac{Q_i^-}{Q_i + Q_i^+ S_{i+1}}, \qquad a_i = -\frac{f_i + Q_i^+ a_{i+1}}{Q_i + Q_i^+ S_{i+1}}. \tag{G.3}$$

For finite recurrences $C_{i>I} = 0$ for some I. To enforce this, we set $S_{I+1} = 0$, $a_{I+1} = 0$ and iterate *downwards* in (G.3) getting all S_i and a_i down to $i = 2$. Now, to reconstruct all C_i from equation (G.2), we only need the anchor C_1, which obeys

$$\left(Q_1 + Q_1^+ S_2 \right) C_1 = -\left(f_1 + Q_1^+ a_2 \right), \tag{G.4}$$

(equation (G.1) at $i = 1$ plus $C_2 = S_2 C_1 + a_2$). Then, starting from the so-obtained C_1, we iterate $C_i = S_i C_{i-1} + a_i$ *upwards*, getting the solution of the recurrence (G.1).

The above is the algorithmic form (easy to implement in a computer). The solution can also be written as $C_i = \left(\prod_{k=2}^{i} S_k \right) C_1 + \sum_{k=2}^{i} \left(\prod_{j=k+1}^{i} S_k \right) a_k$. To illustrate the structure, $C_5 = S_5 S_4 S_3 S_2 C_1 + S_5 S_4 S_3 a_2 + S_5 S_4 a_3 + S_5 a_4 + a_5$. For homogeneous recurrences ($f_i \equiv 0 \Rightarrow a_i = 0$) the solution simply reads $C_i = (S_i S_{i-1} \cdots S_2) C_1$.

As for the name of the method, note that S_i is given in terms of a fraction with S_{i+1} in the denominator, which can in turn be written as a fraction with S_{i+2} in the denominator, and so on. This furnishes the structure of a *continued fraction*

$$C = \frac{p_1}{q_1 + \dfrac{p_2}{q_2 + \cdots}}. \tag{G.5}$$

In simple problems one may identify the continued-fraction representation of some known function [65], getting explicit analytical solutions.

Differential recurrences like $\dot{C}_i = Q_i^- C_{i-1} + Q_i C_i + Q_i^+ C_{i+1} + f_i$ can be handled analogously for t-independent Q_i. Laplace transformation plus $\dot{\tilde{g}}(s) = s\tilde{g}(s) - g(t = 0)$ brings the differential equation into the form $Q_i^- \widetilde{C}_{i-1} + (Q_i - s)\widetilde{C}_i + Q_i^+ \widetilde{C}_{i+1} = -[\widetilde{f}_i + C_i(0)]$. Then, introducing some modified forcings $\hat{f}_i = \widetilde{f}_i + C_i(0)$ and central coefficients $\hat{Q}_i = Q_i - s$ (cf equation (36)) the equation acquires the structure of the ordinary recurrence relation (G.1), and as such can be solved[10].

Further, the quantities in the recursions can be J-vectors (c_i and f_i) with $J \times J$-matrix coefficients $\mathbb{Q}_i$. Then one proceeds analogously: inserting the ansatz $c_i = \mathbb{S}_i c_{i-1} + a_i$ in the recurrence $\mathbb{Q}_i^- c_{i-1} + \mathbb{Q}_i c_i + \mathbb{Q}_i^+ c_{i+1} = -f_i$ and obtaining the coefficients $\mathbb{S}_i$ and shifts a_i, as in equation (G.3). The only change is that the fraction bars stand now for matrix inversion ('from the left' $\mathbb{A}/\mathbb{B} \rightarrow \mathbb{B}^{-1}\mathbb{A}$), and one speaks of *matrix* continued fractions. The algorithm involves I inversions of $J \times J$ matrices, so reducing the storage requirements and number of operations from the direct inversion (or diagonalization) of the underlying $(I \times J) \times (I \times J)$ matrix problem.

In the vector case, to iterate upwards $c_i = \mathbb{S}_i c_{i-1} + a_i$, the initial condition c_1 obeys the matrix version of equation (G.4). In the absence of forcing ($f_i = 0 \Rightarrow a_i = 0$; e.g., the zeroth-order equation (33)) the solution of such $J \times J$ system involves an overall multiplicative constant. One can add an extra equation to fix this, getting an augmented $(J+1) \times J$ system [20, appendix A], which can be solved by methods appropriate for more equations than unknowns (e.g., QR-decomposition), yielding the required c_1. In our spin problems the normalization condition $1 = \sum_n \varrho_{nn} = \sum_n (c_n)_n$ involves all c_n and cannot be used as the extra equation for $c_{n=-S}$ (which plays the role of c_1). However, we can fix arbitrarily one component, e.g., $(c_{-S})_{-S} = $ const (the extra equation) and normalize the solution at the end. A practical choice is a Gibbsian weight $(c_{-S})_{-S} \sim \mathcal{Z}^{-1} \exp(-\varepsilon_{-S}/T)$.

To conclude, as the indices (n, m) can be half-integers (when S is so), we employ in the numerical implementation some integer indices $i = n + (S + 1)$ and $j = m + (S + 1)$, running from 1 to $2S + 1$ $(= I = J)$. For integer S the equations can also be handled as two-sided recurrences $-I \leqslant i \leqslant I$ (then the ansatz and initial conditions are slightly modified; see [4, 20, appendix A]). Although this may enhance stability is some problems, we have used the general protocol allowing for non-integer spins.

References

[1] Weiss U 1993 *Quantum Dissipative Systems* (Singapore: World Scientific)
[2] Guinea F, Bascones E and Calderón M J 1998 *Lectures on the Physics of Highly Correlated Electrons* ed F Mancini (New York: AIP)
[3] Dattagupta S and Puri P 2004 *Dissipative Phenomena in Condensed Matter* (Berlin: Springer)
[4] Risken H 1989 *The Fokker–Planck Equation* 2nd edn (Berlin: Springer)
[5] Balescu R 1997 *Statistical Dynamics* (London: Imperial College Press) (reprinted in 2000)
[6] Caldeira A O and Leggett A J 1983 *Ann. Phys., NY* **149** 374
    Caldeira A O and Leggett A J 1983 *Physica* A **121** 587
[7] Feynman R P and Hibbs A R 1965 *Quantum Mechanics and Path Integrals* (New York: McGraw-Hill) sections 12.7–12.9
[8] Ingold G-L 2002 *Coherent Evolution in Noisy Environments* (*Lecture notes in physics* vol 611) ed A Buchleitner and K Hornberger (Berlin: Springer) pp 1–53 (*Preprint* quant-ph/0208026)
[9] For recent progress on this issue, see Stockburger J T 2003 *Phys. Status Solidi* b **237** 146
[10] Ford G W, Lewis J T and O'Connell R F 1988 *Phys. Rev.* A **37** 4419

---

[10] In general Laplace inversion to get the actual time evolution can be numerically problematic. Here we would have the advantage of (i) the $\widetilde{C}_i(s)$ being numerically exact and (ii) owing to the high efficiency of the continued-fraction method, the possibility of computing them at many s points.

[11] Bhattacharjee J K 2000 *Statistical Physics: Equilibrium and Non-Equilibrium Aspects* (Delhi: Allied Publishers)
[12] Karrlein R and Grabert H 1997 *Phys. Rev.* E **55** 153
[13] Ankerhold J 2003 *Irreversible Quantum Dynamics* (*Lecture notes in physics* vol 622) ed F Benatti and R Floreanini (New York: Springer) p 165 (*Preprint* cond-mat/0309284)
[14] Jung P and Risken H 1985 *Z. Phys.* B **59** 469
     Jung P 1993 *Phys. Rep.* **234** 175
[15] Ferrando R, Spadacini R, Tommei G E and Caratti G 1993 *Physica* A **195** 506
[16] Coffey W T, Kalmykov Yu P and Waldron J T 1994 *Physica* A **208** 462
     Raĭkher Yu L and di Stephanov V 1995 *Phys. Rev.* B **52** 3493
     Kalmykov Yu P and Coffey W T 1997 *Phys. Rev.* B **56** 3325
[17] Lee H-W 1995 *Phys. Rep.* **259** 147
[18] Shibata F and Uchiyama C 1993 *J. Phys. Soc. Japan* **62** 381 see also [56]
[19] Vogel K and Risken H 1988 *Phys. Rev.* A **38** 2409
     Vogel K and Risken H 1989 *Phys. Rev.* A **39** 4675
[20] García-Palacios J L and Zueco D 2004 *J. Phys. A: Math. Gen.* **37** 10735 (*Preprint* cond-mat/0407454)
     García-Palacios J L 2004 *Europhys. Lett.* **65** 735 (*Preprint* cond-mat/0406047)
[21] Anastopoulos C and Halliwell J J 1995 *Phys. Rev.* D **51** 6870
[22] Lindenberg K, Mohanty U and Seshadri V 1983 *Physica* A **119** 1
[23] Jayannavar A M 1991 *Z. Phys.* B **82** 153
[24] García-Palacios J L 1999 *Eur. Phys. J.* B **11** 293
[25] Brown W F Jr 1963 *Phys. Rev.* **130** 1677
[26] Kubo R and Hashitsume N 1970 *Prog. Theor. Phys. Suppl.* **46** 210
[27] Blundell S J and Pratt F L 2004 *J. Phys.: Condens. Matter* **16** R771
[28] Pake G E and Estle T L 1973 *The Physical Principles of Electron Paramagnetic Resonance* 2nd edn (Reading, MA: Benjamin)
[29] Würger A 1998 *J. Phys.: Condens. Matter* **10** 10075
[30] Balucani U, Lee M H and Tognetti V 2003 *Phys. Rep.* **373** 409
[31] Garanin D A 1991 *Physica* A **172** 470
[32] Garanin D A and Chudnovsky E M 1997 *Phys. Rev.* B **56** 11102
[33] White R M 1983 *Quantum Theory of Magnetism* 2nd edn (Berlin: Springer)
[34] Ulyanov V V and Zaslavski O B 1992 *Phys. Rep.* **216** 179
[35] Gamliel D and Levanon H 1995 *Stochastic Processes in Magnetic Resonance* (Singapore: World Scientific)
[36] Dohm V and Fulde P 1975 *Z. Phys.* B **21** 369
[37] Cortés E, West B J and Lindenberg K 1985 *J. Chem. Phys.* **82** 2708
[38] Luis F, Bartolomé J and Fernández J F 1998 *Phys. Rev.* B **57** 505
[39] Pohjola T and Schoeller H 2000 *Phys. Rev.* B **62** 15026
[40] Hu B L, Paz J P and Zhang Y 1992 *Phys. Rev.* D **45** 2843
[41] Kohler S, Dittrich T and Hänggi P 1997 *Phys. Rev.* E **55** 300
[42] Cataldo H M 1990 *Physica* A **165** 249
[43] Desposito M A and Hernandez E S 1995 *J. Phys. A: Math. Gen.* **28** 775
[44] Garanin D A 1997 *Phys. Rev.* E **55** 2569
[45] Garanin D A, Ishchenko V V and Panina L V 1990 *Theor. Math. Phys. (USSR)* **82** 169
[46] Lindenberg K and Seshadri V 1981 *Physica* A **109** 483
[47] Zueco D and García-Palacios J L 2006 *Phys. Rev.* B **73** 104448 (*Preprint* cond-mat/0509627)
[48] Dattagupta S 1987 *Relaxation Phenomena in Condensed Matter Physics* (Orlando: Academic)
[49] García-Palacios J L and Svedlindh P 2000 *Phys. Rev. Lett.* **85** 3724
[50] Raĭkher Yu L and di Stephanov V 1997 *Phys. Rev.* B **55** 15 005
[51] Haydock R 1980 *Solid State Phys.* **35** 215
     Finnis M 2003 *Interatomic Forces in Condensed Matter* (Oxford: Oxford University Press) section 7.9
[52] Bender C M and Milton K A 1994 *J. Math. Phys.* **35** 364
[53] Allegrini M, Arimondo E and Bambini A 1977 *Phys. Rev.* A **15** 718
[54] Narducci L M, Bowden C M, Bluemel V and Carrazana G P 1975 *Phys. Rev.* A **11** 280
[55] Carlin R L 1986 *Magnetochemistry* (Berlin: Springer)
[56] Shibata F 1980 *J. Phys. Soc. Japan* **49** 15
     Shibata F and Asou M 1980 *J. Phys. Soc. Japan* **49** 1234
     Asou M and Shibata F 1981 *J. Phys. Soc. Japan* **50** 1846
     Asou M and Shibata F 1981 *J. Phys. Soc. Japan* **50** 2481
[57] Böttcher C J F and Bordewijk P 1978 *Theory of Electric Polarization* vol 2 (Amsterdam: Elsevier)

[58] García-Palacios J L and Dattagupta S 2005 *Phys. Rev. Lett.* **95** 190401 (*Preprint* quant-ph/0505002)
[59] Garanin D A 1996 *Phys. Rev.* E **54** 3250 and references cited herein
[60] Barra A-L *et al* 1996 *Europhys. Lett.* **35** 133
[61] Gomes A M *et al* 1998 *Phys. Rev.* B **57** 5021
[62] Spohn H 1980 *Rev. Mod. Phys.* **52** 569
[63] Blanga L D and Despósito M A 1996 *Physica* A **227** 248
[64] Munro W J and Gardiner C W 1996 *Phys. Rev.* A **53** 2633
[65] Wall H S 1973 *Analytic Theory of Continued Fractions* (New York: Chelsea) (reprint)